Synthesis and Decomposition of Alkyl Complexes of Molybdenum(IV) That Contain a $[(Me_3SiNCH_2CH_2)_3N]^{3-}$ Ligand. Direct Detection of α-Elimination Processes That Are More than Six Orders of Magnitude Faster than β-Elimination Processes

Richard R. Schrock,*,† Scott W. Seidel,† Nadia C. Mösch-Zanetti,† Keng-Yu Shih,† Myra B. O'Donoghue,† William M. Davis,† and William M. Reiff‡

Contribution from the Departments of Chemistry, Massachusetts Institute of Technology, Cambridge, Massachusetts 02139, and Northeastern University, Boston, Massashusetts 02115

Received March 4, 1997[⊗]

Abstract: A variety of paramagnetic molybdenum complexes, $[N_3N]MoR$ ($[N_3N]^{3-} = [(Me_3SiNCH_2CH_2)_3N]^{3-}$; R = Me, Et, Bu, CH_2Ph, CH_2SiMe_3, CH_2CMe_3, cyclopropyl, cyclobutyl, cyclopentyl, cyclohexyl, cyclopentenyl, phenyl), have been prepared from $[N_3N]MoCl$. The several that have been examined all follow Curie−Weiss $S = 1$ behavior with a magnetic moment in the solid state between 2.4 and 2.9 μ_B down to 50 K. Below ∼50 K the effective moments undergo a sharp decrease as a consequence of what are proposed to be a combination of spin−orbit coupling and zero field splitting effects. NMR spectra are temperature dependent as a consequence of "locking" of the backbone into one C_3-symmetric conformation and as a consequence of Curie−Weiss behavior. The cyclopentyl and cyclohexyl complexes show another type of temperature-dependent fluxional behavior that can be ascribed to a rapid and reversible α-elimination process. For the cyclopentyl complex the rate constant for α-elimination is $\sim 10^3$ s^{-1} at room temperature, while the rate constant for α-elimination for the cyclohexyl complex is estimated to be ∼200 s^{-1} at room temperature. An isotope effect for α-elimination for the cyclohexyl complex was found to be ∼3 at 337 K. Several of the alkyl complexes decompose between 50 and 120 °C. Of the complexes that contain linear alkyls, only $[N_3N]Mo(CH_2CMe_3)$ decomposes cleanly (but slowly) by α,α-dehydrogenation to give $[N_3N]Mo{\equiv}CCMe_3$. $[N_3N]MoMe$ is by far the most stable of the alkyl complexes; no $[N_3N]Mo{\equiv}CH$ can be detected upon attempted thermolysis at 120 °C. Other decompositions of linear alkyl complexes are complicated by competing reactions, including β-hydride elimination. β-Hydride elimination (to give $[N_3N]MoH$) is the sole mode of decomposition of the cyclopentyl and cyclohexyl complexes; the former decomposes at a rate calculated to be approximately 10× that of the latter at 298 K. β-Hydride elimination in $[N_3N]Mo$(cyclopentyl) to give (unobservable) $[N_3N]Mo$(cyclopentene)(H) has been shown to be 6−7 orders of magnitude slower than α-hydride elimination to give (unobservable) $[N_3N]Mo$(cyclopentylidene)(H). $[N_3N]Mo$(cyclopropyl) evolves ethylene in a first-order process upon being heated to give $[N_3N]Mo{\equiv}CH$, while $[N_3N]Mo$(cyclobutyl) is converted into $[N_3N]Mo{\equiv}CCH_2CH_2CH_3$. $[N_3N]MoH$ decomposes slowly and reversibly at 100 °C to yield molecular hydrogen and $[(Me_3SiNCH_2CH_2)_2NCH_2CH_2SiMe_2CH_2]Mo$ ($[bitN_3N]Mo$). X-ray structures of $[N_3N]Mo$(triflate), $[N_3N]MoMe$, $[N_3N]Mo$(cyclohexyl), and $[bitN_3N]Mo$ show that the degree of twist of the TMS groups away from an "upright" position correlates with the size of the ligand in the apical pocket and that steric congestion in the cyclohexyl complex is significantly greater than in the methyl complex. Relief of steric strain in the ground state in molecules of this general type to give a less crowded alkylidene hydride intermediate is proposed to be an important feature of the high rate of α-elimination relative to β-elimination in several circumstances.

Introduction

Triamidoamine ligands, $[(RNCH_2CH_2)_3N]$,$^{3-}$ in which R is a bulky substituent, can bind to a variety of transition metals[1] (or main group elements[2]), especially in oxidation states 3+ or higher. The synthesis of the pentane-soluble trilithium salt[3] of $(Me_3SiNHCH_2CH_2)_3N$[4] allowed the chemistry of complexes containing the $[(Me_3SiNCH_2CH_2)_3N]^{3-}$ ($[N_3N]^{3-}$) ligand to develop relatively rapidly. (The only other ligand that has been employed to prepare a significant number of triamidoamine transition metal complexes is $[(C_6F_5NCH_2CH_2)_3N]^{3-}$.[1,5]) Triamidoamine ligands usually bind to a transition metal in a tetradentate manner, thereby creating a sterically protected, 3-fold-symmetric "pocket" in which only three orbitals are available to bond to additional ligands in that pocket, two degenerate π orbitals (approximately d_{xz} and d_{yz}) and a σ orbital (approximately d_{z^2}). This frontier orbital picture contrasts sharply with that for the ubiquitous bent metallocene in which all three orbitals (two with A_1 symmetry and one with B_2 symmetry in the C_{2v} point group) lie *in* the plane passing between the two Cp rings.[6] The fact that the two frontier π orbitals in a C_3-symmetric triamidoamine complex are strictly degenerate and probably essentially pure d orbitals creates an

† Massachusetts Institute of Technology.
‡ Northeastern University.
⊗ Abstract published in *Advance ACS Abstracts,* November 15, 1997.

(1) Schrock, R. R. *Acc. Chem. Res.* **1997**, *90*, 99.
(2) Verkade, J. G. *Acc. Chem. Res* **1993**, *26*, 483.
(3) Cummins, C. C.; Schrock, R. R.; Davis, W. M. *Organometallics* **1992**, *11*, 1452.
(4) Gudat, D.; Verkade, J. G. *Organometallics* **1989**, *8*, 2772.
(5) Kol, M.; Schrock, R. R.; Kempe, R.; Davis, W. M. *J. Am. Chem. Soc.* **1994**, *116*, 4382.
(6) Albright, T. A.; Burdett, J. K.; Whangbo, M.-H. *Orbital Interactions in Chemistry*; Wiley & Sons: New York, 1985.

S0002-7863(97)00697-5 CCC: $14.00

Table 1. Selected Distances (Å) and Angles (deg) for Structurally Characterized Compounds

	$[N_3N]MoCl$[a]	$[N_3N]Mo(OTf)$	$[N_3N]Mo(CD_3)$	$[N_3N]Mo(Cy)$	$[bitN_3N]Mo$
Mo−L_{ax}	2.398(2)	2.166(8)	2.188(11)	2.167(14)	2.249(3)
Mo−N(1)	1.976(3)	1.974(8)	1.984(9)	1.991(7)	1.948(2)
Mo−N(2)	1.976(3)	1.977(7)	1.996(9)	2.012(7)	1.983(2)
Mo−N(3)	1.976(3)	1.980(8)	1.973(10)	1.987(7)	1.994(2)
Mo−N(4)	2.185(5)	2.171(9)	2.303(9)	2.422(10)	2.237(2)
Mo−N(1)−Si(1)	128.2(2)	129.8(5)	128.0(5)	128.2(4)	102.30(10)
Mo−N(2)−Si(2)	128.2(2)	130.7(5)	129.1(5)	126.4(4)	127.08(10)
Mo−N(3)−Si(3)	128.2(2)	126.2(5)	127.1(5)	131.9(4)	125.87(11)
N(1)−Mo−N(2)	117.7(1)	116.6(3)	117.2(4)	116.3(3)	116.95(8)
N(2)−Mo−N(3)	117.7(1)	117.9(3)	117.6(4)	113.9(3)	116.83(8)
N(1)−Mo−N(3)	117.7(1)	118.3(3)	116.4(4)	116.1(3)	118.27(8)
N(4)−Mo−N(1)−Si(1)	176.6[b]	136.1[b]	162.4[b]	129.1[b]	176.1[b]
N(4)−Mo−N(2)−Si(2)	176.6[b]	141.4[b]	163.3[b]	131.3[b]	178.9[b]
N(4)−Mo−N(3)−Si(3)	176.6[b]	142.6[b]	160.0[b]	135.9[b]	170.9[b]
N(1)−Mo−L_{ax}	98.8[b]	103.4[b]	99.9(4)	105.8(3)	76.13(9)
N(2)−Mo−L_{ax}	98.8[b]	97.7[b]	99.3(4)	102.0(3)	110.04(9)
N(3)−Mo−L_{ax}	98.8[b]	95.8[b]	100.7(4)	99.6(3)	110.68(11)
Mo−O(1)−S		156.9(5)			
Mo−C(101)−C(102)				120.0(7)	
Mo−C(101)−C(106)				116.9(7)	
Mo−C(11)−Si(1)					88.35(10)
C(11)−Si(1)−N(1)					92.93(11)
N(4)−Mo−C(11)					155.16(8)

[a] See ref 15. [b] Obtained from a Chem 3D model.

environment that is especially favorable for formation of a metal−ligand triple bond.

We have been interested in the chemistry of Mo and W triamidoamine complexes from several perspectives, including dinitrogen fixation,[5,7,8] terminal phosphido and arsenido complexes,[9−11] and new organometallic chemistry.[7,12,13] In this paper, we report the synthesis, characterization, and decomposition of a variety of alkyl complexes of molybdenum that contain the $[(Me_3SiNCH_2CH_2)_3N]^{3-}$ ($[N_3N]^{3-}$) ligand. Among the unusual reactions reported here are dehydrogenation of $[N_3N]MoCH_2R'$ complexes to give $[N_3N]Mo{\equiv}CR'$ complexes and cleavage of C−C bonds in cyclopropyl and cyclobutyl complexes to give alkylidyne complexes. We also have been presented with the opportunity to prove that α-elimination reactions are faster than *β*-elimination reactions for cyclopentyl and cyclohexyl complexes, even though the products of α-elimination (alkylidene hydrides) and *β*-elimination (olefin hydrides) are not observable. Some of these results have been reported in a preliminary fashion.[7,13] These results should be compared with those obtained for related tungsten complexes,[12,13] the full details of which will be reported elsewhere.[14]

Results

Chloride and Triflate Complexes. Addition of $MoCl_4(THF)_2$ to $Li_3[N_3N]$ in THF yields paramagnetic $[N_3N]MoCl$ (**1a**) in a maximum yield of ∼40%. Many variations of this reaction have been attempted in an effort to increase the yield, but so far without success. We suspect that loss of Me_3SiCl or reduction of Mo(IV) is a persistent problem, in part because related reactions between $(C_6F_5NHCH_2CH_2)_3N$ and $MoCl_4(THF)_2$ in the presence of NEt_3 give $[(C_6F_5NCH_2CH_2)_3N]MoCl$ in high yield.[5] The reaction between $Li_3[N_3N]$ and $MoCl_3(THF)_3$ also gives **1a** in a yield of ∼25%. Similar results have been reported by Verkade.[15] Red $[N_3N]Mo(OTf)$ (**1b**) can be prepared in ∼62% yield by treating $[N_3N]MoCl$ with $[Cp_2Fe]OTf$ in dichloromethane. We anticipated that the metal center in $[N_3N]Mo(OTf)$ would be more electrophilic than that in $[N_3N]MoCl$, possibly rendering it more suitable for some reactions. However, in reactions of the type discussed in this paper, $[N_3N]MoCl$ has been a reproducibly accessible and satisfactory starting material.

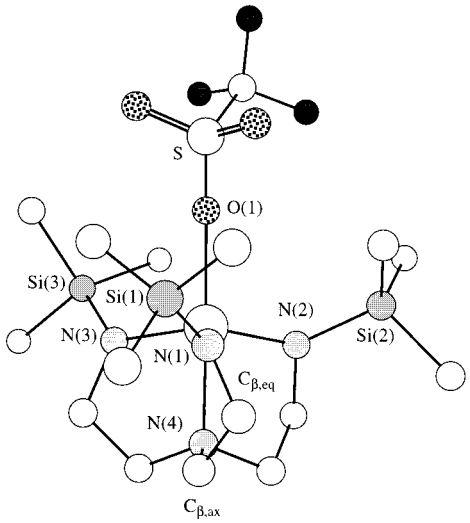

Figure 1. View of the structure of $[N_3N]Mo(triflate)$.

It is instructive to compare the structure of $[N_3N]Mo(OTf)$ (as determined in an X-ray study; Figure 1, Table 1) with the published structure of $[N_3N]MoCl$,[15] selected bond distances and angles for which are also listed in Table 1. The structure of $[N_3N]MoCl$ shows that the TMS groups are all oriented "upright," i.e., the N_{ax}−Mo−N_{eq}−Si dihedral angles are all

(7) Shih, K.-Y.; Schrock, R. R.; Kempe, R. *J. Am. Chem. Soc.* **1994**, *116*, 8804.
(8) O'Donoghue, M. B.; Zanetti, N. C.; Schrock, R. R.; Davis, W. M. *J. Am. Chem. Soc.* **1997**, *119*, 2753.
(9) Zanetti, N. C.; Schrock, R. R.; Davis, W. M. *Angew. Chem., Int. Ed. Engl.* **1995**, *34*, 2044.
(10) Johnson-Carr, J. A.; Zanetti, N. C.; Schrock, R. R.; Hopkins, M. D. *J. Am. Chem. Soc.* **1996**, *118*, 11305.
(11) Wu, G.; Rovnyak, K.; Johnson, M. J. A.; Zanetti, N. C.; Musaev, D. G.; Morokuma, K.; Schrock, R. R.; Griffin, R. G.; Cummins, C. C. *J. Am. Chem. Soc.* **1996**, *118*, 10654.
(12) Shih, K.-Y.; Totland, K.; Seidel, S. W.; Schrock, R. R. *J. Am. Chem. Soc.* **1994**, *116*, 12103.
(13) Schrock, R. R.; Shih, K.-Y.; Dobbs, D.; Davis, W. M. *J. Am. Chem. Soc.* **1995**, *117*, 6609.
(14) Schrock, R. R.; Dobbs, D. A.; Seidel, S. W.; Mösch-Zanetti, N. C.; Shih, K.-Y.; Davis, W. M. *Organometallics*, in press.
(15) Duan, Z.; Verkade, J. G. *Inorg. Chem.* **1995**, *34*, 1576.

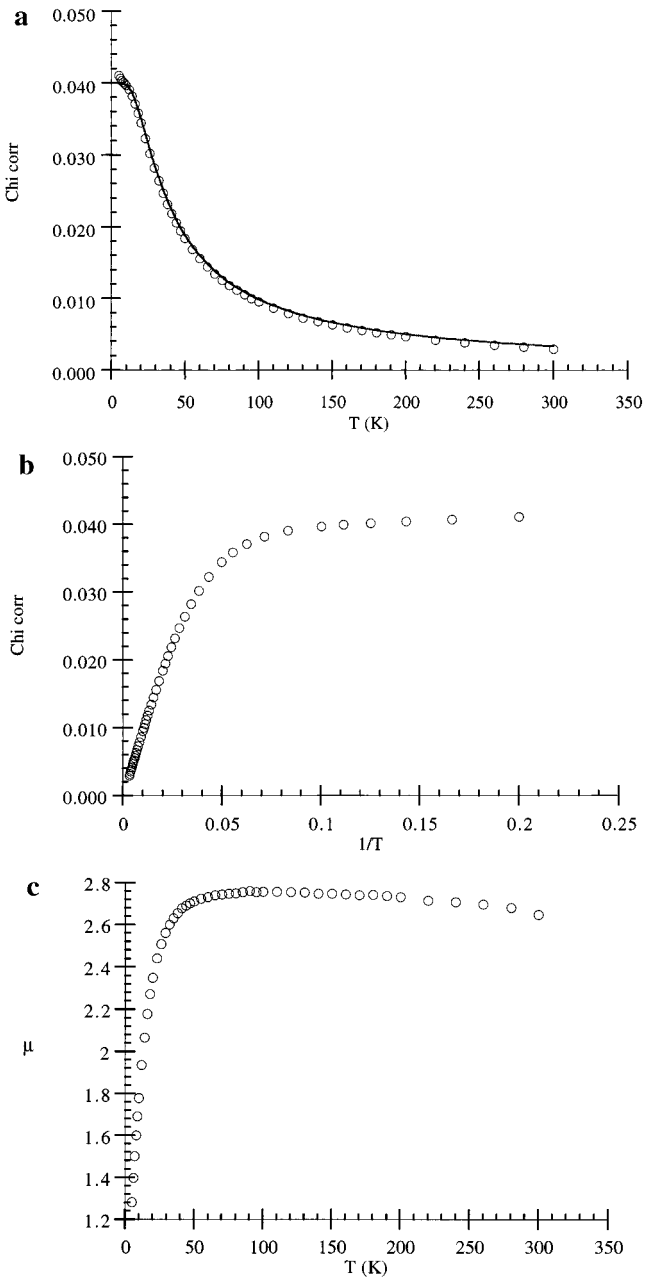

Figure 2. (a) Plot of χ versus T for $[N_3N]MoCl$. (b) Plot of χ versus $1/T$ for $[N_3N]MoCl$. (c) Plot of μ_{eff} versus T for $[N_3N]MoCl$.

176.6°, as a consequence of $C_{\beta,ax}$ (see Figure 1) serving as the "flap" in an "envelope" configuration of the MoN_2C_2 five-membered ring. The only significant difference between the structures of $[N_3N]Mo(OTf)$ and $[N_3N]MoCl$ is that the $N_{ax}-Mo-N_{eq}-Si$ dihedral angles in $[N_3N]Mo(OTf)$ are much smaller than 180° (136−143°) as a consequence of $C_{\beta,eq}$ serving as the "flap" in the MoN_2C_2 five-membered ring (Figure 1). We speculate that the steric bulk of the triflate ligand causes the trimethylsilyl groups in $[N_3N]Mo(OTf)$ to "twist" and that this is the most facile response to a sterically bulky ligand in the apical pocket. A significant increase in the $Mo-N_{eq}-Si$ angles, which is another possible way to relieve steric problems,[7] is likely to be more costly energetically. The structures of compounds to be discussed later confirm that the degree of "twist" of the trimethylsilyl groups correlates with the size of the ligand in the apical pocket.

The magnetic susceptibility of $[N_3N]MoCl$ (plotted versus T in Figure 2a and versus $1/T$ in Figure 2b) approaches a constant, and μ_{eff} decreases sharply (Figure 2c) as the temperature approaches 5 K. However, a plot of the susceptibility above 50 K versus T can be fit to a curve defined by a Curie−Weiss equation ($\chi = \mu^2/8(T + \theta)$) to give values of $\mu = 2.92$ and $\theta = 6.4$. (The error in μ is estimated to be ±0.10 and in θ to be ±1 K.) These data suggest that $[N_3N]MoCl$ is a Curie−Weiss paramagnet between room temperature and ∼50 K in the solid state with μ_{eff} essentially the spin only value expected for d^2 Mo(IV). We assume that the two electrons are in the set of degenerate nonbonding orbitals of π symmetry (approximately d_{xz} and d_{yz} if $N_{ax}-Mo-Cl$ is taken to be the z axis). The susceptibility of $[N_3N]MoCl$ in the solid state between 6 and 300 K was mentioned in another publication,[15] but only Curie−Weiss behavior above 100 K ($\mu_{eff} = 2.35$, $\theta = 0.148$ K) was noted.

The fairly abrupt decrease in the effective magnetic moment below ∼50 K can be attributed to a combination of spin−orbit effects and low-symmetry ligand field components that result in zero field splitting of the d^2 ground-state spin triplet.[16] If the d^2 complex were an undistorted octahedron with *no* low-symmetry ligand field components and a $^3T_{1g}$ ground state, the ambient-temperature magnetic moment might reflect a substantial orbital contribution above spin-only (λ-negative) or might actually be somewhat less than the latter for λ-positive, where the magnitude of these effects depends on the magnitude of λ relative to k_BT. In this context, the moments for undistorted d^2 systems will generally *gradually decrease* with temperature with depopulation of the nine spin−orbit states of $^3T_{1g}$ (A). In the limit of low symmetry (e.g., the C_3 or C_{3v} environments of the present complexes), the orbital degeneracy of the ground and all excited states is largely removed, leading to ambient temperature moments closer to spin-only, regardless of the sign or magnitude of λ (at least for Mo). The temperature variation of μ or χ can be described in terms of a formalism[17,18] that emphasizes the axial zero field splitting (D) of the ground spin manifold. Using this formalism, the observed susceptibility of $[N_3N]MoCl$ could be modeled ($R = 0.9995$) over the entire range of temperatures and a D value of $+35$ cm^{-1} obtained assuming a value of $E = 0.1$ (where E is the rhombic splitting parameter) and $g_x = g_y = g_z = 2$ (Figure 2a). All d^2 Mo compounds of the $[N_3N]MoX$ type that we have examined here show a variation of susceptibility with temperature similar to that observed for $[N_3N]MoCl$. Since $\lambda(W^{4+}) \sim 1050$ cm^{-1} while $\lambda(Mo^{4+}) \sim 475$ cm^{-1},[16] spin−orbit effects are larger for the W^{4+} analogues.[14] Consequently $[N_3N]WX$ species have reduced moments of ∼2 μ_B near room temperature and a susceptibility that changes relatively little (compared to that for the analogous $[N_3N]MoX$ species) as the temperature is lowered.[14]

The proton NMR spectrum of $[N_3N]MoCl$ consists of three broadened, shifted resonances, one for the TMS groups and two for the backbone methylene protons of the $[N_3N]^{3-}$ ligand, consistent with a paramagnetic species that has C_{3v} symmetry on the NMR time scale. It is not known with certainty which of the two methylene resonances observed at higher temperatures can be ascribed to which $[N_3N]^{3-}$ backbone methylene group. As the temperature of the NMR sample is lowered the spectrum changes in two ways. First, the methylene resonances shift upfield (Figure 3a) and the TMS resonance shifts (to a lesser extent) downfield (not shown). If the chemical shift of each methylene proton set is plotted versus $1/T$, then nearly linear plots are obtained (Figure 3b), as expected for a Curie−Weiss

(16) Figgis, B. N.; Lewis, J. *Prog. Inorg. Chem.* **1964**, *6*, 37.
(17) Oosterhuis, W. T.; Dockum, B.; Reiff, W. M. *J. Chem. Phys.* **1977**, *67*, 3537.
(18) Reiff, W. M.; Wong, H.; Baldwin, J. E.; Huff, J. *Inorg. Chim. Acta* **1977**, *25*, 91.

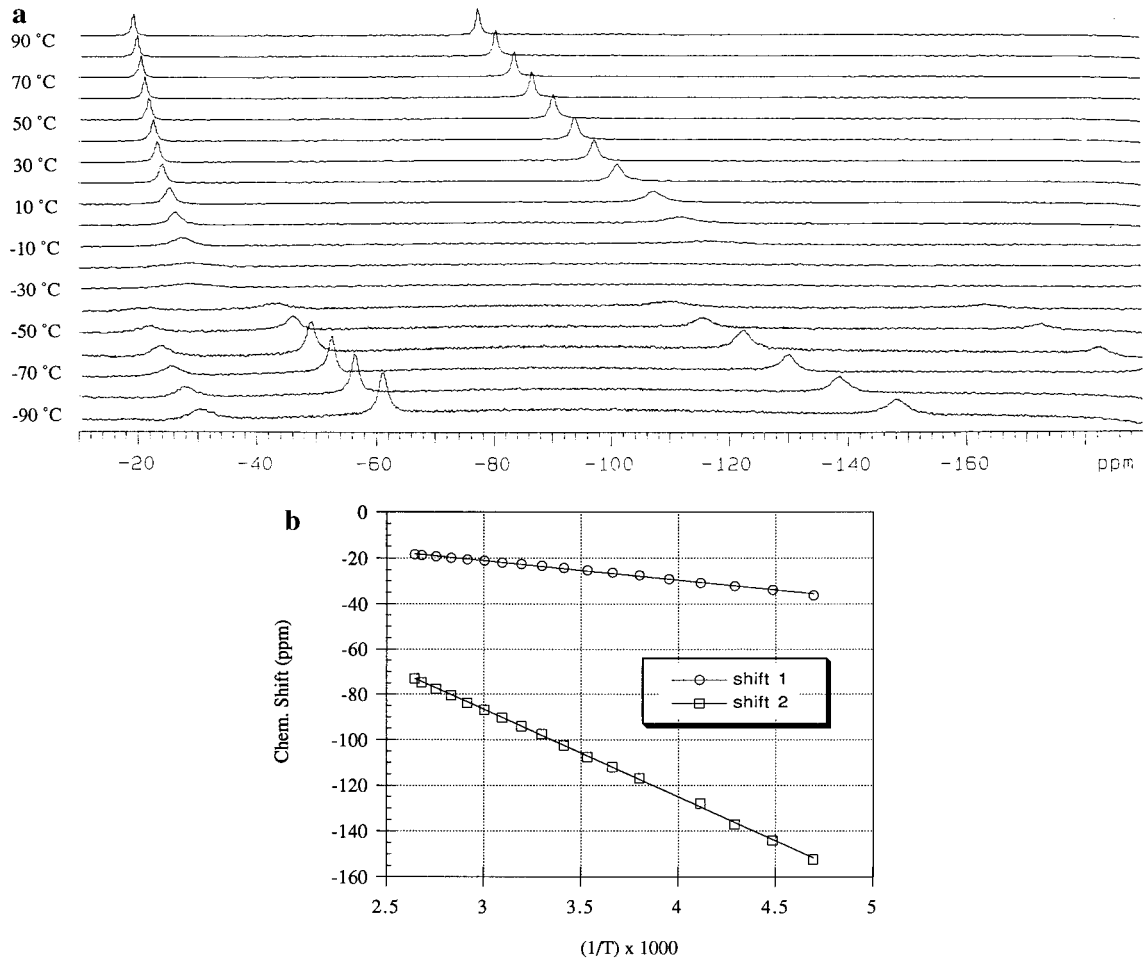

Figure 3. (a) Variable-temperature 500 MHz proton NMR spectra of $[N_3N]MoCl$ in toluene-d_8. (b) Plot of the chemical shift of the methylene backbone resonances versus $1/T$.

paramagnet in solution in this temperature range. (The average of the two methylene resonances below the coalescence point discussed below was employed whenever possible in Figure 3b.) The second temperature-dependent process that is observed is a "locking" of the three MoN_2C_2 rings in the ligand backbone at the lowest temperatures to give a species that has one C_3-symmetric conformation, e.g., the one in which $C_{\beta,eq}$ is the "flap" of the envelope (as in $[N_3N]Mo$(triflate); see above), the one in which $C_{\beta,ax}$ is the "flap" of the envelope (as in $[N_3N]MoCl$[15]), or some conformation between the two (as in $[N_3N]Mo(CD_3$; see below). At higher temperatures the C_3-symmetric species becomes C_{3v}-symmetric on the NMR time scale as a consequence of the MoN_2C_2 rings "flipping" rapidly between the two chiral forms. Using the chemical shift difference between the two types of backbone protons at a temperature that is as close as possible to the temperature of coalescence, an approximate $\Delta G^{\ddagger}$ for the C_{3v}/C_3 fluxional process was calculated to be 9.2 kcal/mol at ∼−30 °C and 9.0 kcal/mol at ∼−20 °C. (The errors in these values are estimated to be at least ± 0.2 kcal mol^{-1}.) A C_{3v}/C_3 fluxional process is observed for all $[N_3N]MoX$ species discussed in this paper. A C_{3v}/C_3 fluxional process is also observed for a variety of other C_{3v} symmetric metal complexes that contain the $[N_3N]^{3-}$ ligand, including diamagnetic species,[1] and for complexes that contain the $[(C_6F_5NCH_2CH_2)_3N]^{3-}$ ligand.[19] We assume that the apical nitrogen donor does not have to dissociate from the metal for the C_{3v}/C_3 fluxional process to occur. We have not attempted in any systematic way to correlate $\Delta G^{\ddagger}$ for the C_{3v}/C_3 fluxional process with the nature of the ligand in the apical pocket.

(19) Seidel, S. W.; Reid, S. M. Unpublished results.

Molybdenum−Alkyl Complexes. Several *n*-alkyl and cycloalkyl complexes, a 1-cyclopentenyl complex, and a phenyl complex were prepared by treating $[N_3N]MoCl$ with lithium reagents, as shown in eq 1. Several complexes could be isolated

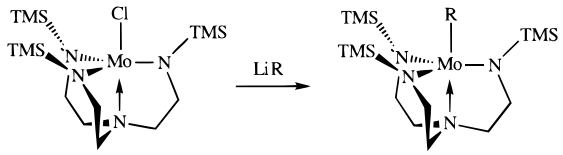

(1)

R = Me (**2a**), Et (**2b**), Bu (**2c**), CH_2Ph (**2d**), CH_2SiMe_3 (**2e**), CH_2CMe_3 (**2f**), cyclopropyl (**2g**), cyclobutyl (**2h**), cyclopentyl (**2i**), cyclohexyl (**2j**), cyclopentenyl (**2k**), or phenyl (**2l**)

in only ∼50% yield as a consequence of their high solubility in hydrocarbon solvents. Compounds **2k,l** are also paramagnetic, i.e., conjugation of the olefinic or aromatic π systems with the metal is insufficient to break the d_{xz}/d_{yz} degeneracy. Many of these compounds are purple with a relatively weak transition near 500 nm (e.g., $\epsilon = 680$ M^{-1} cm^{-1} at 480 nm for $[N_3N]MoMe$ in toluene; see the Experimental Section for other compounds). However, the benzyl, trimethylsilyl, and neopentyl complexes have visible spectra that show an additional, increasingly strong absorption shifted to lower energy (Figure 4). The visible spectrum of the neopentyl complex shows the strongest low-energy absorption at ∼688 nm. The neopentyl complex consequently is green-black instead of purple. We suspect that these absorptions arise from "d−d" transitions (e.g., d_{xz}/d_{yz} to $d_{x^2-y^2}/d_{xy}$) and speculate that increasingly significant distortions

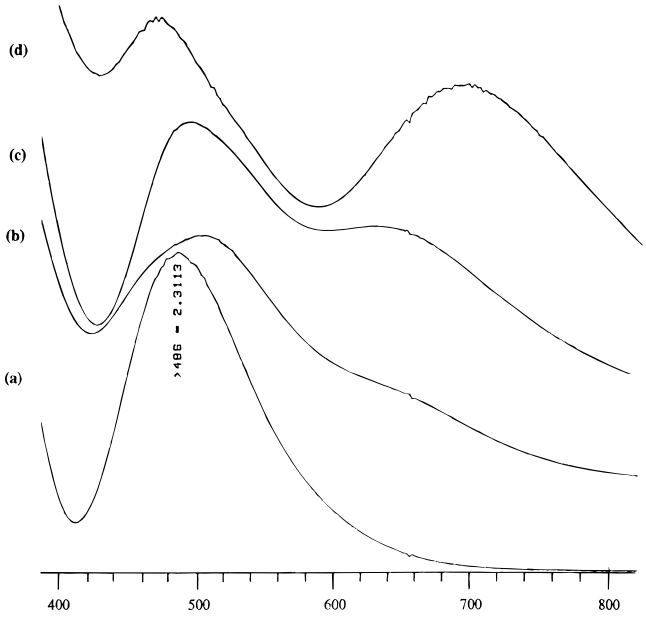

Figure 4. UV/vis spectra of $[N_3N]MoR$ complexes in toluene: R = (a) Me; (b) CH_2Ph; (c) CH_2SiMe_3; (d) CH_2CMe_3.

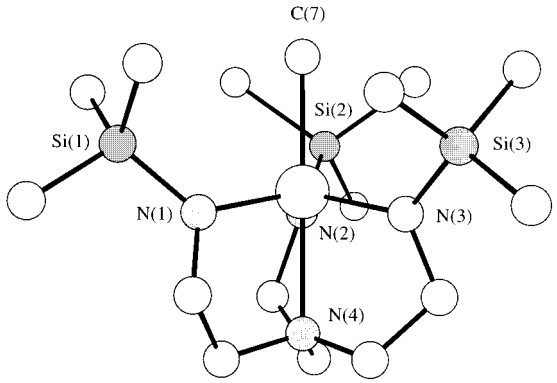

Figure 5. View of the structure of $[N_3N]Mo(CD_3)$.

of the MoN_4 core when a bulky CH_2R ligand is present in the apical position lead to a splitting of orbitals that are degenerate in C_{3v} symmetry and to new lower energy absorptions. Detailed studies clearly will be required to elucidate the origin of this behavior fully and possibly to correlate any structural distortions with altered magnetic behavior.

A view of the structure of $[N_3N]Mo(CD_3)$, as determined in an X-ray study, is shown in Figure 5, and bond distances and angles are compared with distances and angles in other compounds in Table 1. (The choice of the CD_3 over the CH_3 complex was circumstantial.) The structure of $[N_3N]Mo(CD_3)$ is most similar to that of $[N_3N]MoCl$, except the TMS groups are twisted slightly (N(4)−Mo−N−Si angles of 160−163°) and both $C_{\beta,eq}$ and $C_{\beta,ax}$ deviate from a given $MoN_{ax}N_{eq}$ plane. This configuration of a MoN_2C_2 five-membered ring is between that in the "upright" and "twisted" forms referred to above for $[N_3N]$-MoCl and $[N_3N]Mo(OTf)$, respectively. The long Mo−N(4) distance (2.303(9) Å) could be ascribed to the metal being less electrophilic in $[N_3N]Mo(CD_3)$ than in $[N_3N]MoCl$ (Mo−N(4) = 2.185(5) Å) or $[N_3N]Mo(OTf)$ (Mo−N(4) = 2.171(9) Å). We propose that the TMS groups are twisted to a greater degree in $[N_3N]MoMe$ than in $[N_3N]MoCl$ as a consequence of the slightly larger methyl ligand being present in the apical pocket.

A drawing of the structure of $[N_3N]Mo$(cyclohexyl) is shown in Figure 6. (See Table 1 for selected distances and angles.) The cyclohexyl ring is oriented so that it lies roughly in a plane that passes between N(1) and N(3) and between N(1) and N(2).

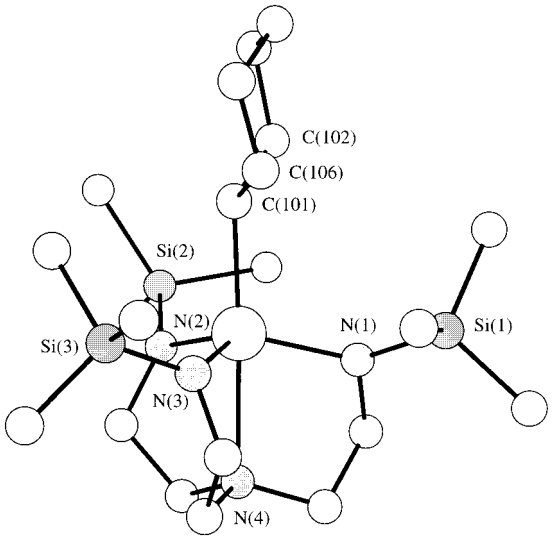

Figure 6. View of the sttructure of $[N_3N]Mo$(cyclohexyl).

Table 2. Values of μ_{eff} in the Solid State for $[N_3N]MoX$ Compounds[a]

compd	μ_{eff}	θ (K)
$[N_3N]MoCl$	2.92	6.4
$[N_3N]MoMe$	2.76 (2.61)	11.1 (4.8)
$[N_3N]Mo(CH_2SiMe_3)$	2.72 (2.78)	3.8 (7.5)
$[N_3N]Mo$(cyclopentyl)	2.58 (2.60)	−2.2 (−2.4)
$[N_3N]MoD$	2.79	−2.5
$[bitN_3N]Mo$	2.46 (2.78)	0.8 (2.12)

[a] Obtained from SQUID data between 5 and 300 K by fitting the corrected susceptibility between 50 and 300 K to the equation $\chi = \mu^2/8(T + \theta)$. The error in μ is estimated to be ±0.10 and in θ to be ±1. Numbers in parentheses refer to a second sample.

The Mo−C(101) distance (2.167(14) Å) is the same as Mo−C(7) in $[N_3N]Mo(CD_3)$. The Mo−C(101)−C(106) and Mo−C(101)−C(102) angles (117−120°) are larger than tetrahedral, consistent with a significant amount of steric pressure within the trigonal pocket. The possibility of any concomitant α agostic[20,21] interaction between the C(101)−H_α bond and the metal seems remote in view of the fact that the only available orbitals (d_{xz} and d_{yz}) each contain one electron. Interestingly, the N(4)−Mo−N_{eq}−Si dihedral angles are all dramatically smaller than found in $[N_3N]Mo(CD_3)$ (smaller even than in $[N_3N]Mo(OTf)$) and the Mo−N(4) distance is approximately 0.1 Å longer than in $[N_3N]Mo(CD_3)$. We propose that both are consistent with a significantly greater degree of steric interaction between the cyclohexyl ring and the silyl groups on the equatorial amido nitrogens. "Steric pressure" within the pocket in $[N_3N]Mo$(alkyl) complexes could sharply distinguish one complex from another in terms of visible spectra (as proposed above) or, as we shall see shortly, in terms of the ease of some proton elimination processes.

The susceptibilities of $[N_3N]MoMe$, $[N_3N]Mo(CH_2SiMe_3)$, and $[N_3N]Mo$(cyclopentyl) in the solid state vary with temperature in ways that are entirely analogous to the behavior of the susceptibility of $[N_3N]MoCl$ versus temperature. Results for $[N_3N]MoMe$ and $[N_3N]Mo$(cyclopentyl) are shown, along with the susceptibility of two compounds to be discussed later, in

(20) Brookhart, M.; Green, M. L. H.; Wong, L. *Prog. Inorg. Chem.* **1988**, *36*, 1.

(21) (a) Maus, D. C.; Copié, V.; Sun, B.; Griffiths, J. M.; Griffin, R. G.; Luo, S.; Schrock, R. R.; Liu, A. H.; Seidel, S. W.; Davis, W. M.; Grohmann, A. *J. Am. Chem. Soc.* **1996**, *118*, 5665. (b) Bell, A.; Clegg, W.; Dyer, P. W.; Elsegood, M. R. J.; Gibson, V. C.; Marshall, E. L. *J. Chem. Soc., Chem. Commun.* **1994**, 2547. (c) Casty, G. L.; Tilley, T. D.; Yap, G. P. A.; Rheingold, A. L. *Organometallics* **1997**, *16*, 4746.

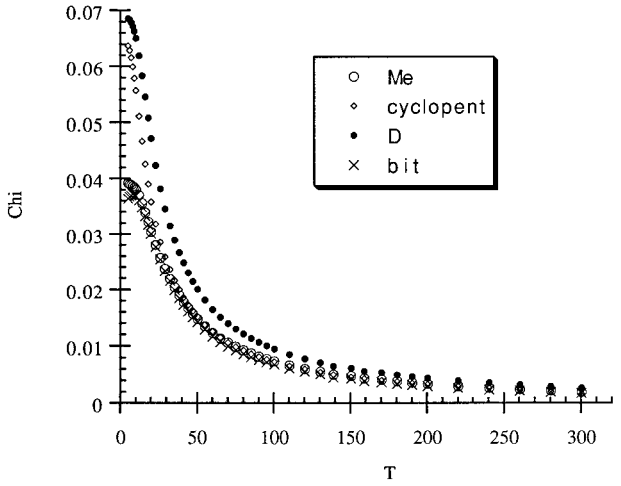

Figure 7. Plot of χ versus T for [N_3N]MoMe, [N_3N]Mo(cyclopentyl), [N_3N]MoD, and [bitN_3N]Mo.

Figure 7. In Table 2 are shown values for μ and θ determined from a fit of the data above 50 K to a Curie−Weiss law. The magnetic moment for [N_3N]MoMe in C_6D_6 at 25 °C was found to be 2.9 μ_B by the Evan's method, consistent with the results obtained in the solid state, and with an $S = 1$ spin ground state.

NMR spectra of [N_3N]MoR species show broadened and shifted ligand resonances and variable-temperature behavior that is analogous to that noted for N_3N]MoCl (Figure 3a). For example, the high-field portion of the spectrum of [N_3N]MoMe that contains resonances for the backbone methylene protons is shown in Figure 8a. As the temperature is lowered the two ligand methylene resonances shift to higher field in a linear fashion versus $1/T$ (Figure 8b). Values for $\Delta G^{\ddagger}$ for the C_{3v}/C_3 fluxional process that becomes slow on the NMR time scale at ∼−60 °C in [N_3N]Mo(CH_3) can be calculated as described for [N_3N]MoCl; values thus calculated are 8.6 and 8.2 kcal mol^{-1}. (We estimate the error to be at least ±0.2 kcal mol^{-1} for each.) These values for $\Delta G^{\ddagger}$ are close to those found for [N_3N]MoCl (9.0 and 9.2 kcal/mol). Therefore it does not appear, according to these data, that activation energies for the C_3/C_{3v} fluxional processes in different compounds in this general family of [N_3N]-Mo complexes differ dramatically.

So far we have not been able to observe an α proton resonance in any [N_3N]MoR complex. To be certain that we did not overlook an α-proton resonance, we searched for a ^{2}H resonance in [N_3N]Mo(CD_3) between +400 and −400 ppm. (We chose ^{2}H NMR because resonances in ^{2}H NMR spectra of paramagnetic compounds are often significantly narrower than those in ^{1}H NMR spectra and, therefore, are more readily observed in paramagnetic complexes.[22]) However, we could observe no ^{2}H resonance that could be ascribed to the CD_3 group in [N_3N]Mo(CD_3), even after hours of collection time at 76.7 MHz. We conclude that either the CD_3 resonance in [N_3N]-Mo(CD_3) is outside the +400 to −400 ppm region or its intensity is virtually nil using the standard methods of data collection that we have employed so far, or both. In no other [N_3N]Mo(alkyl) species discussed here have we been able to observe any ^{1}H or ^{2}H resonance for protons or deuterons on a carbon directly bound to Mo.

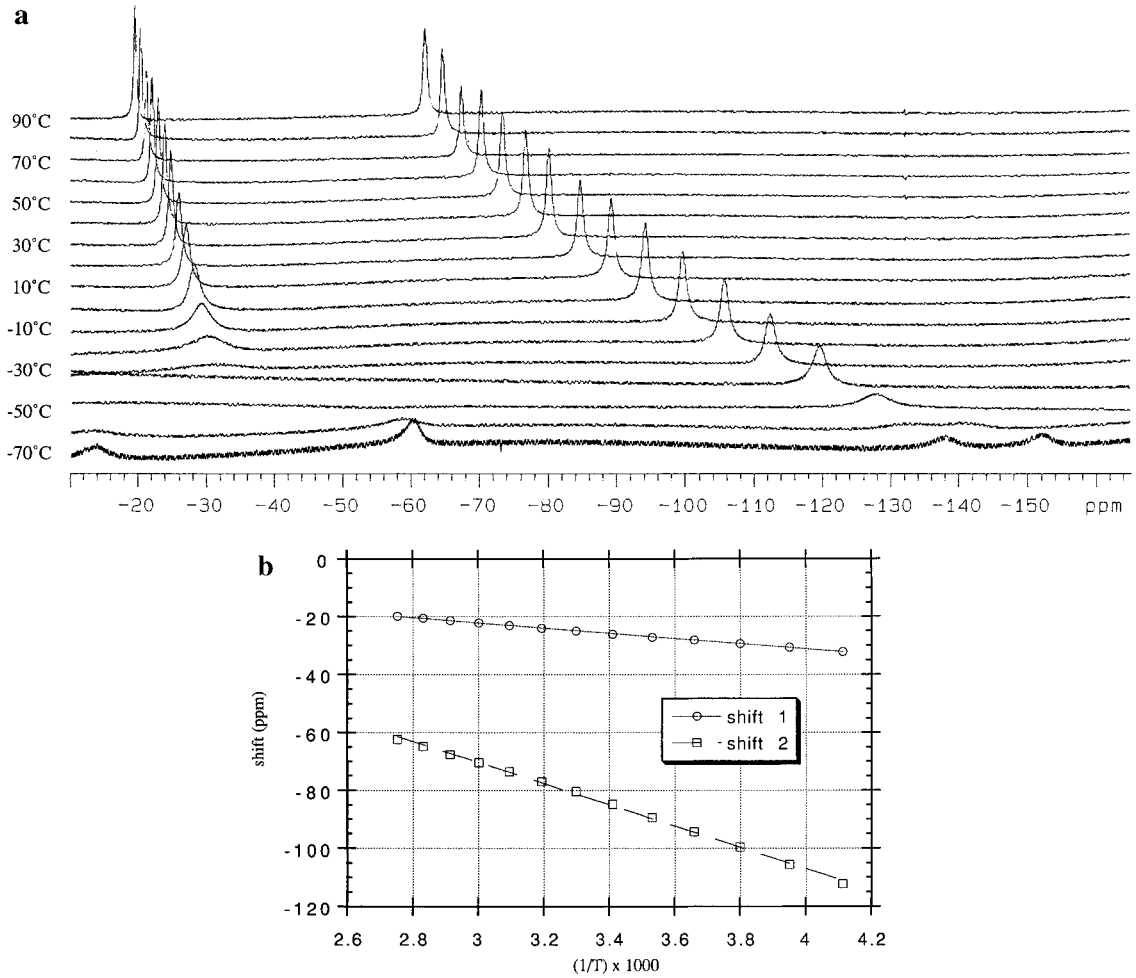

Figure 8. (a) Variable-temperature 500 MHz proton NMR spectra of the ligand backbond resonances in [N_3N]MoMe. (b) Plot of the chemical shift of the methylene backbone resonances versus $1/T$.

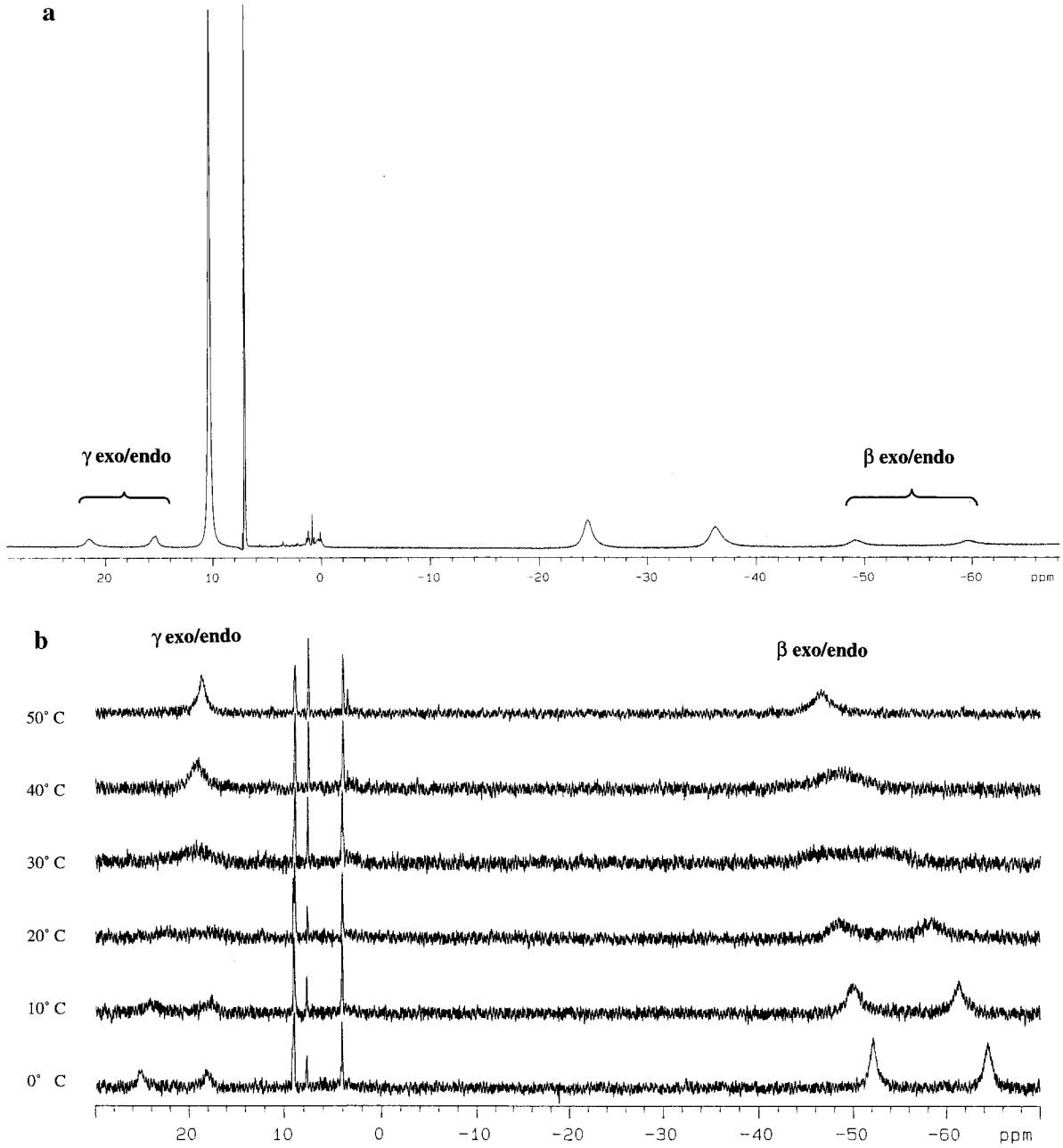

Figure 9. (a) 500 MHz ^{1}H NMR spectrum of [N_3N]Mo(C_5H_9) at 22 °C. (b) Variable-temperature 76.7 MHz ^{2}H NMR spectra of [N_3N]Mo(C_5H_8D).

Resonances for protons on the β-carbon of an alkyl ligand can be observed, however. For example, the ^{1}H NMR spectrum of [N_3N]Mo(CH_2CH_3) shows a broad resonance at −51.5 ppm (at 22 °C), in addition to temperature-dependent resonances that can be ascribed to the TMS groups and two types of ligand backbone methylene protons, as described earlier for analogous species. β-Proton resonances in other alkyl complexes (see below) are also typically found in the range −50 to −60 ppm. The position of the β-proton resonances also depends on temperature, as expected for a Curie−Weiss paramagnetic species, moving to higher field at lower temperatures.

The variable-temperature ^{1}H NMR spectrum of [N_3N]Mo(CH_2-$CH_2CH_2CH_3$) between 60 and −60 °C shows (in addition to the TMS and backbone methylene resonances) three resonances (at 22 °C) at −48, +2.9, and +5.4 ppm. The resonance at −48 ppm can be assigned to the β methylene protons, while the resonances at +2.9 and +5.4 ppm can be assigned to the γ and δ proton resonances, or vice versa. The only temperature-dependent processes observed in the range +60 to −60 °C are the Curie 1/T chemical shift dependence and "locking" of the ligand backbone to give a species with C_3 symmetry at low temperatures.

The ^{1}H NMR spectrum of [N_3N]Mo(cyclopentyl) shows four broadened and shifted resonances for cyclopentyl ligand protons at 21.3, 15.6, −48.2, and −58.3 ppm at 22 °C (Figure 9a). On the basis of chemical shift, the resonances at 21.3 and 15.6 ppm can be ascribed to exo and endo γ-protons (without specifying which is which), endo protons being defined as those on the same side of the ring as the metal, while those at −48.2 and −58.3 ppm can be ascribed to exo and endo β-protons (again without being able to specify which is endo and which is exo). The H_α proton resonance is not observable, and at low temperatures, the ligand backbone becomes locked in a C_3-symmetric configuration.

The ^{2}H NMR spectrum of [N_3N]Mo(cyclopentyl-α-*d*) (prepared by adding Li(cyclopentyl-α-*d*) to [N_3N]MoCl and isolated

(22) *NMR of Paramagnetic Molecules*; LaMar, G. N., Horrocks, W. D., Jr., Holm, R. H., Ed.; Academic: New York, 1973.

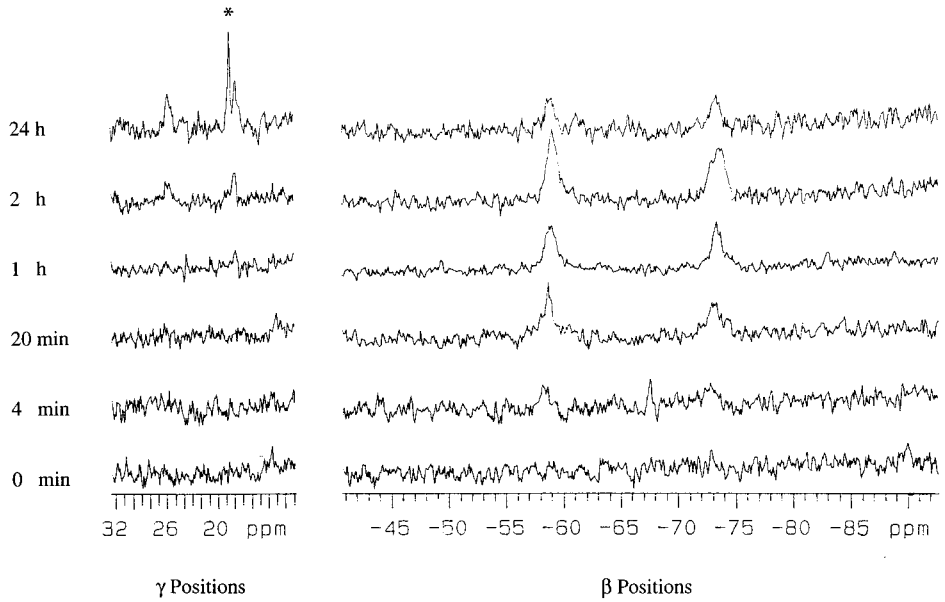

Figure 10. 46.02 MHz ^{2}H NMR spectra (at −20 °C) of [N_3N]Mo(α-C_5H_8D) as a function of the time the sample was kept at 25 °C. (* A resonance for natural abundant ^{2}H in the TMS group of [N_3N]MoH, a decomposition product; see text.)

in a normal workup procedure at room temperature; Figure 9b) revealed *four* broad resonances for $^2H_{\gamma,exo}$ and $^2H_{\gamma,endo}$ (or vice versa) and $^2H_{\beta,exo}$ and $^2H_{\beta,endo}$ (or vice versa) at the same chemical shifts (at a given temperature) as found in the ^{1}H NMR spectrum of [N_3N]Mo(cyclopentyl) (Figure 9a). They are best observed when the sample is cooled to 0 °C for reasons that will be discussed below. These data confirm that the one deuterium has washed into all exo and endo β and γ cyclopentyl positions. (We assume at this stage that residual $^2H_\alpha$ is also present but is not observable.) When [N_3N]Mo(cyclopentyl-α-*d*) was prepared by adding Li(cyclopentyl-α-*d*) to [N_3N]MoCl in toluene at −20 °C and the sealed sample was monitored by ^{2}H NMR, the results shown in Figure 10 were obtained. Initially only a resonance for the deuterium in Li(cyclopentyl-α-*d*) was observed at 0.6 ppm. (Alkylation is relatively slow at −20 °C in toluene.) The sample was then warmed for brief periods to 25 °C and cooled to −20 °C to record the ^{2}H NMR spectrum. After a total of ∼10 min at 25 °C all Li(cyclopentyl-α-*d*) had been consumed. However, at this stage, only weak $^2H_\beta$ resonances were observed (at −20 °C) at −58 and −72 ppm. No γ-resonances were observed near 20 ppm. The intensity of the β-resonances increased with time, reaching a maximum after the sample had stood for a total of 1−2 h at room temperature. After 2 h some γ-deuteron intensity was observed near 20 ppm. After 24 h the spectrum clearly revealed resonances at 18 and 27 ppm (at −20 °C) for ^{2}H in γ-positions (Figure 10). The resonances at 18 and 27 ppm are slightly less intense than those at −58 and −72 ppm, probably as a consequence of the rapidly decreasing rate of incorporation into γ-positions for statistical reasons, as only one ^{2}H total is present. (The γ-resonances in the sample whose ^{2}H NMR spectrum is shown in Figure 9b are also much less intense than the β-resonances, as this solid sample had been kept at −30 °C after being isolated at 25 °C.) Therefore we can say confidently that α-D in [N_3N]Mo(cyclopentyl-α-*d*) washes into the β,exo *and* β,endo positions of the cyclopentyl ring *before* it washes into the γ,exo *and* γ,endo positions.

The mechanism by which D appears on a β-carbon in an *exo* position is proposed to be the well-known β-hydride elimination (eq 2). (We will show later that loss of cyclopentene from intermediate [N_3N]Mo(cyclopentene)(H) is relatively slow and irreversible under these conditions.) Subsequent β-hydride

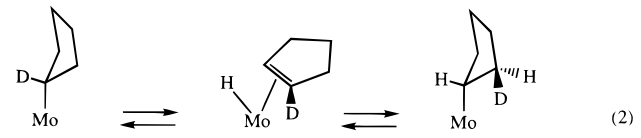

(2)

elimination would yield the species in which D appears on a γ-carbon in an *exo* position. However, if *only* β-hydride elimination were taking place, D would appear *only* in exo positions (eq 3). Therefore another faster process must inter-

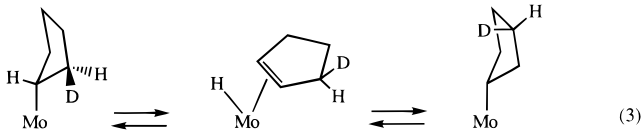

(3)

convert exo and endo protons on β- and γ-carbons. (This faster process is discussed below.) We can estimate from Figure 10 that scrambling of ^{2}H from the α carbon to the β carbons in both exo and endo positions is complete (∼5 half-lives) in 60−120 min. Therefore the half-life for appearance of D in a β-position is between 12 and 24 min at 22 °C or $k_\beta = \sim 5 \times 10^{-4}$ s^{-1} to $\sim 10^{-3}$ s^{-1}. No significant cyclopentene is lost from the cyclopentene hydride intermediate under these conditions. (We show later that at 66 °C $t_{1/2} = 17$ min for cyclopentene elimination.) At equilibrium one-ninth of one deuterium should be found at each of the nine cyclopentyl positions, ignoring any equilibrium isotope effects and assuming that D is scrambled relatively rapidly between exo and endo positions by some other process.

^{2}H NMR spectra of [N_3N]Mo(cyclopentyl-α-*d*) from 0 to 50 °C (Figure 9b) reveal that exo and endo deuterons equilibrate rapidly on the NMR time scale at the higher temperatures, where decomposition to give [N_3N]MoH (see later) is still slow. The four broad resonances observed at low *T* coalesce to two average resonances that shift toward the diamagnetic region of the spectrum as a consequence of their Curie dependence on 1/*T*. This behavior is entirely reversible. (The sharp resonances between 4 and 9 ppm in Figure 9b are due to naturally abundant ^{2}H in the toluene solvent and the small amount of cyclopentene-d_1 formed upon decomposition of [N_3N]Mo(cyclopentyl-d_1) at the higher temperatures.) This fluxional process cannot be observed unambiguously by ^{1}H NMR for several reasons, among

them the factor of 6.5 difference between ^1H and ^2H frequencies. Note that the fluxional process that leads to interconversion of exo and endo ^2H *cannot involve any* α-^2H in the averaging process. If $^2H_\alpha$ were scrambling rapidly with γ- or β-protons, then the resulting average resonance would be either shifted significantly or decreased in intensity dramatically, or both. Instead, $^2H_{\beta,exo}$ averages with $^2H_{\beta,endo}$, $^2H_{\gamma,exo}$ averages with $^2H_{\gamma,endo}$, and the average $^2H_\beta$ and $^2H_\gamma$ resonances shift toward the diamagnetic region as the temperature approaches 50 °C. The fluxional process is not consistent with any slowed rotation of the cyclopentyl ring within the trigonal pocket, as the backbone still has pseudo C_{3v} symmetry at a temperature where the cyclopentyl ^2H ring resonances are resolved (0 °C in the ^1H NMR spectrum.)

We propose that the fluxional process that leads to averaging of exo and endo ^2H on C_β and exo and endo ^2H on C_γ consists of *a rapid and reversible* α-elimination to give an intermediate [N_3N]Mo(cyclopentylidene)(H) complex (eq 4). This unusual

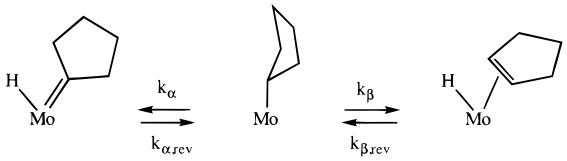

(4)

proposal is sensible in view of the fact that an attempt to prepare [N_3N]W(cyclopentyl) yielded crystallographically characterized [N_3N]W(cyclopentylidene)(H) instead.[13] The rate constant for α-elimination (k_α) at 22 °C can be estimated to be 10^3 (from NMR experiments), while the half-life for β-elimination can be estimated to be between 12 ($k = 5 \times 10^{-4}$ s^{-1}) and 24 ($k = 10^{-3}$ s^{-1}) min at 22 °C (see above). Therefore we can say that the rate constant for α-elimination is *at least 6 orders of magnitude larger* than the rate constant for β-elimination at room temperature, i.e., $k_\alpha > 10^6\, k_\beta$ (eq 4). (An accurate comparison of the rate constants for α- and β-elimination per C−H bond would have to include a factor of 2 for statistical reasons, but we need not consider that adjustment here in view of the magnitude of the rate differences in question.) We assume that [N_3N]Mo(cyclopentylidene)(H), like [N_3N]W(cyclopentylidene)-(H),[13] is diamagnetic and that [N_3N]Mo(cyclopentene)(H) also would be diamagnetic. There is no evidence that suggests that any significant amount of either is present, i.e., the equilibria for both α- and β-elimination lie well toward [N_3N]Mo-(cyclopentyl). If we assume that the equilibrium constants for forming [N_3N]Mo(cyclopentyl) ($k_{\alpha,rev}/k_\alpha$ and $k_{\beta,rev}/k_\beta$) are both ∼10^2 (or greater), then $k_{\beta,rev} \approx 10^{-1}$ s^{-1} (or greater) and $k_{\alpha,rev} \approx 10^5$ s^{-1} (or greater). An alternative explanation of the phenomenon of interconversion of exo and endo cyclopentyl protons involves C−C bond cleavage and formation of a 1-molybdacyclohexene complex that has mirror symmetry, but rapid and reversible C−C bond cleavage would seem to be much less likely than rapid and reversible C−H bond cleavage. (See also the Discussion.) It should be noted that a significant primary H/D kinetic isotope effect might be expected for an α-elimination process,[23] but since only one ^2H is present among eight ^1H nuclei in the sample whose ^2H NMR spectrum is shown in Figure 9b, we are observing a virtually pure $^1H_\alpha$ elimination in this case.

The ^1H NMR spectrum of [N_3N]Mo(cyclohexyl) (Figure 11a) shows six resonances for the cyclohexyl ring exo and endo protons that average upon heating the sample. [N_3N]Mo-(cyclohexyl) is more stable than [N_3N]Mo(cyclopentyl), so it is possible to heat it to higher temperatures before it decomposes to [N_3N]MoH and cyclohexene (see below). Nevertheless, resonances for [N_3N]MoH complicate the study, as do other resonances for [N_3N]Mo(cyclohexyl). We assign the resonances at 15.8 and 6.1 ppm to exo and endo γ-protons, those at 1.9 and −2.0 ppm to exo and endo δ-protons, and those at −40.9 and −49.9 ppm to exo and endo β-protons. Interference by other resonances and the breadth of the cyclohexyl β-, γ-, and δ-resonances in the ^1H NMR spectrum of [N_3N]Mo(cyclohexyl) makes these results less convincing than those for [N_3N]Mo-(cyclopentyl-d_1). Nevertheless, we can observe coalescence of the δ-proton resonances at 64 ± 2 °C (shown in Figure 11a) and the β-resonances at ∼100 °C (less accurately and not shown). Unfortunately, the γ-resonances coalesce under the broad resonance for the TMS group in [N_3N]Mo(cyclohexyl) at ∼10 ppm. From coalescence of exo and endo δ-protons we can obtain an approximate value for $k_{\alpha,C6}$ (2×10^3 s^{-1}) at 64 °C. This value should be compared with the value for k_α in the cyclopentyl complex, $k_{\alpha,C5} \approx 10^3$ s^{-1} at 22 °C. At 64 °C, $k_{\alpha,C5}$ perhaps would be $\sim 16 \times 10^3$, or approximately eight times larger than $k_{\alpha,C6}$. (Another estimate at a different temperature is possible using another approach below.) Note that in the cyclohexyl case it is possible to distinguish a rapid α elimination from a rapid β-elimination on the basis of the number of average resonances alone (three ideally), regardless of assignment.

The ^2H NMR spectrum of [N_3N]Mo(C_6D_{11}) at 46.02 MHz is shown in Figure 11b. The expected six C_6D_{11} resonances in the ratio of 2(γ):2(γ):1(δ):1(δ):2(β):2(β) are observed at 10 °C. Upon heating the sample these resonances broaden and coalesce pairwise. The coalescence temperature varies for each set of resonances as a consequence of the different chemical shift difference between the respective exo and endo ^2H resonances ($\gamma > \beta > \delta$). But since a single physical process (α-elimination) is responsible for all coalescence phenomena, we can obtain a rate for that process at three different temperatures from the spectrum shown in 11b. The results for a ∼0.1 M sample in toluene are $k_\alpha = 378$ s^{-1} at 324 K, 755 s^{-1} at 339 K, and 955 s^{-1} at 343 K. Virtually identical values were obtained for a sample that was one-half the concentration (0.05 M). By performing a similar experiment at 76.7 MHz three additional points were obtained: $k_\alpha = 606$ s^{-1} at 331 K, 1273 s^{-1} at 346 K, and 1555 s^{-1} at 352 K. A plot of ln(k/T) versus $1/T$ for these six points gave $\Delta H^\ddagger = 11(1)$ kcal mol^{-1} and $\Delta S^\ddagger = -14$-(3) e.u. (Exact values may be found in the Experimental Section.) From the data shown in Figure 11a a value for the rate constant for α-elimination in [N_3N]Mo(C_6H_{11}) at 337 K was found to be 2155 s^{-1}. Since the rate of α-elimination in [N_3N]Mo(C_6D_{11}) at 337 K can be calculated to be 696 s^{-1}, k_H/k_D for α-elimination at 337 K is 3.1. (We estimate the error (σ) in k_H/k_D to be at least ±0.5.) Observation of a substantial isotope effect confirms that a C−H bond cleavage is involved in the process that gives rise to interconversion of exo and endo protons and, therefore, rules out a possible, if implausible, alternative equilibration by C−C bond cleavage and formation of a metallacycloheptene ring. We also can compare the rate constant for α-elimination at 22 °C for [N_3N]Mo(C_6D_{11}) (calculated to be ∼64 s^{-1}) and [N_3N]Mo(C_5H_9) (estimated to be ∼1000 s^{-1}). The k_α at 22 °C for [N_3N]Mo(C_6H_{11}) should be ∼200 s^{-1} on the basis of $k_H/k_D \approx 3$. The rate of α-elimination in [N_3N]Mo(C_5H_9) is approximately 5 times faster than the rate of α-elimination in [N_3N]Mo(C_6H_{11}) at 22 °C (cf. the estimate of 8 times faster at 64 °C above).

Both [N_3N]Mo(cyclobutyl) and [N_3N](cyclopropyl) have been studied by variable-temperature ^1H NMR to determine if a similar rapid α-elimination process is occurring. The endo and

(23) Schrock, R. R. In *Reactions of Coordinated Ligands*; P. R. Braterman, Ed.; Plenum: New York, 1986.

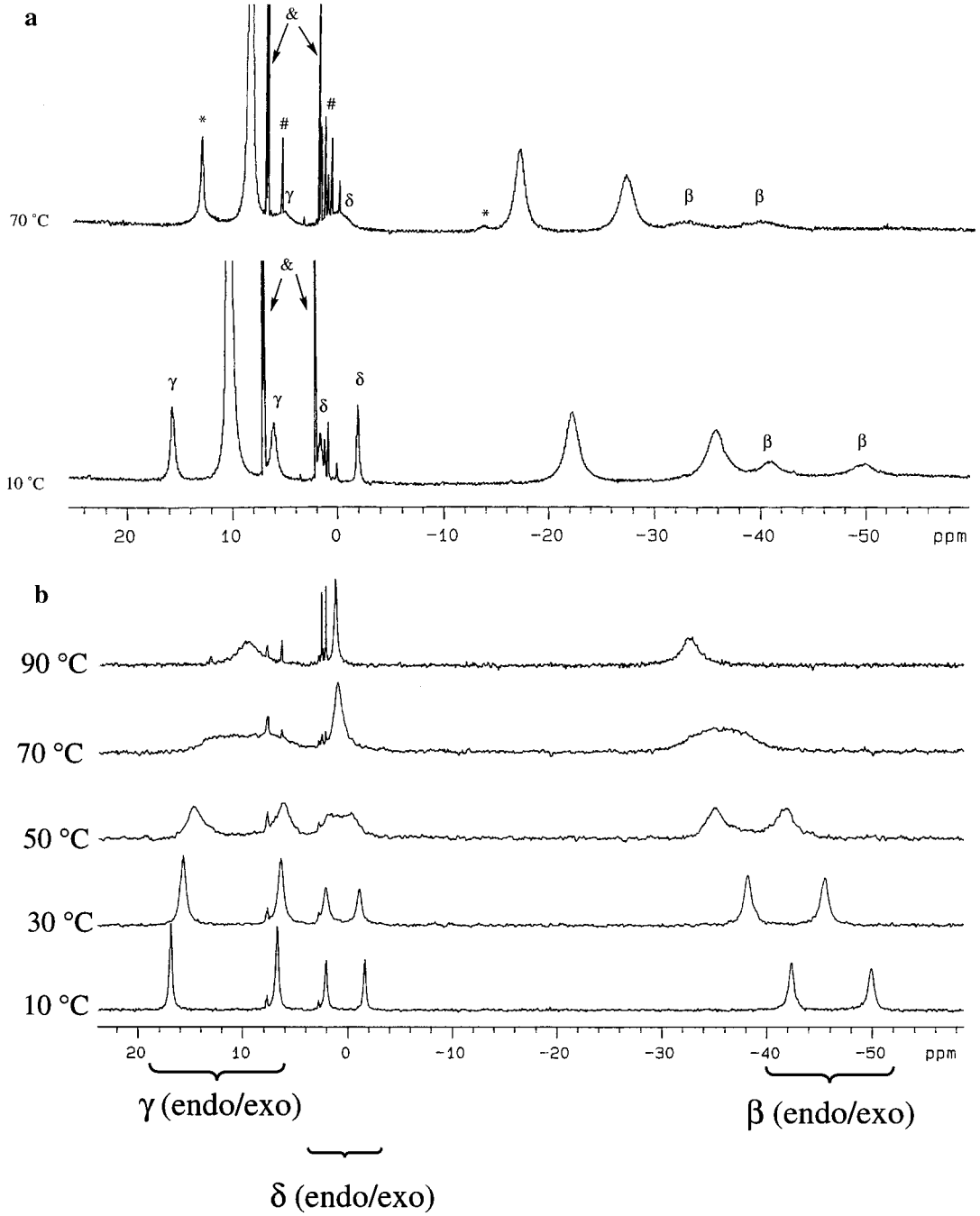

Figure 11. (a) 300 MHz ^{1}H NMR spectra of $[N_3N]Mo(C_6H_{11})$ at two temperatures. Peaks labeled β, γ, and δ are due the cyclohexyl ring protons. Peaks labeled with * are due to $[N_3N]MoH$, which is formed relatively rapidly at 70 °C. Peaks labeled # are due to cyclohexene, the other product resulting from thermolysis of $[N_3N]Mo(C_6H_{11})$. The & indicates the residual protonated toluene resonances. (b) The 46.02 MHz variable-T ^{2}H NMR spectrum of $[N_3N]Mo(C_6D_{11})$.

exo β-protons in the cyclopropyl complex are separated by >110 ppm. A value of 110 ppm would require too high a temperature to observe coalescence, since the cyclopropyl complex decomposes to $[N_3N]Mo{\equiv}CH$ with a half-life of ~1 h at 50 °C (see below). In $[N_3N]Mo$(cyclobutyl), the endo and exo γ-protons are too close to each other and broad to evaluate whether they indeed coalesce. (As the sample is warmed, the resonances simply shift to give one broad resonance, presumably as a consequence of Curie 1/T dependence.) Therefore we cannot confirm or exclude a reversible α-elimination process in $[N_3N]$-Mo(cyclobutyl) and $[N_3N]$(cyclopropyl) at this stage.

Decomposition of Molybdenum−Alkyl Complexes. When solutions of $[N_3N]Mo(CH_2$-t-Bu) in toluene are heated, dihydrogen is lost and $[N_3N]Mo{\equiv}C$-t-Bu (**3f**) is formed quantitatively in a first-order reaction (eq 5). This conversion can be

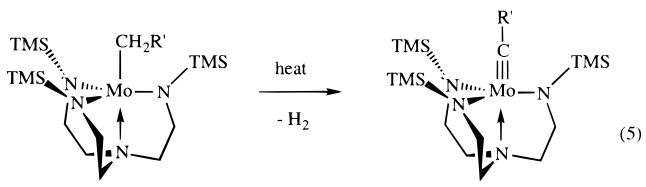

(5)

R' = TMS (**3e**), t-Bu, (**3f**)

followed conveniently by visible spectroscopy by monitoring the decrease in intensity of the absorption at either 480 or 688 nm (Figure 4), since the alkylidyne complex does not absorb significantly in this region. The rate was measured in toluene at four temperatures from 90 to 121 °C (see the Experimental Section) and from a plot of ln(k/T) versus 1/T $\Delta H^{\ddagger}$ was found to be 26.0 kcal mol^{-1} and $\Delta S^{\ddagger}$ to be −7 eu (Table 3). A

Table 3. $\Delta H^{\ddagger}$ and $\Delta S^{\ddagger}$ Values for Decomposition of Alkyls Obtained via UV/Vis Kinetic Techniques

	$\Delta H^{\ddagger}$ (kcal mol^{-1})[a]	$\Delta S^{\ddagger}$ (eu)[b]	k (341 K) (10^{-4} s^{-1})[c]	k (298 K) (10^{-6} s^{-1})[c]
[N_3N]Mo(neopentyl) (**2f**) in toluene	26.0	−7	0.042	0.014
[N_3N]Mo(cyclopropyl) (**2g**) in toluene	21.5	−9	10.0	8.8
[N_3N]Mo(cyclopropyl) (**2g**) in THF	21.4	−10	7.7	7.0
[N_3N]Mo(cyclobutyl) (**2h**) in toluene	24.4	0	14.5	6.9
[N_3N]Mo(cyclopentyl) (**2i**) in toluene	21.6	−10	6.2	5.3
[N_3N]Mo(cyclohexyl) (**2j**) in toluene	24.5	−5	0.86	0.40

[a] Error ≈ 0.2 kcal. [b] Error ≈ 1 eu. [c] Calculated from exact values for $\Delta H^{\ddagger}$ and $\Delta S^{\ddagger}$ given in the Experimental Section.

characteristic low-field resonance for the alkylidyne carbon atom[24] in [N_3N]Mo≡C-*t*-Bu was observed at 316.1 ppm. [N_3N]Mo(CH_2SiMe_3) decomposes much more slowly than [N_3N]Mo(CH_2CMe_3), and the decomposition is more complicated. After 2 days in toluene-d_8 at 100 °C a sample of [N_3N]Mo(CH_2SiMe_3) had only partially decomposed to two diamagnetic products, a C_3-symmetric species and an C_s-symmetric species that contains characteristic resonances at 12.1 (triplet) and 4.55 (doublet) ppm in a ratio of 1:2. After 5 days at 100 °C only the C_3-symmetric species was clearly visible in solution in a yield (versus an internal standard) of ∼30%. Although the low yield prevented confirmation by ^{13}C NMR that the C_3-symmetric species is [N_3N]Mo≡$CSiMe_3$, the chemical shifts of the proton NMR resonances in the [N_3N]$^{3-}$ ligand are virtually identical with those for well-characterized alkylidyne complexes of this type ([N_3N]Mo≡CH and [N_3N]Mo≡CPr below). Evidently the unidentified C_s-symmetric species is not stable at 100 °C, while [N_3N]Mo≡$CSiMe_3$, like other alkylidyne complexes in this category, is stable at 100 °C. Although the complex nature of the decomposition of [N_3N]Mo(CH_2SiMe_3) to [N_3N]Mo≡$CSiMe_3$ prevented measurement of a meaningful half-life, we estimate it to be ∼48 h at 100 °C. For comparison, the half-life of [N_3N]Mo(CH_2CMe_3) at 100 °C is ∼1.4 h. We prefer not to speculate on the nature of the unstable C_s-symmetric species formed in this decomposition reaction.

[N_3N]Mo(CH_2Ph) decomposes even more slowly than [N_3N]Mo(CH_2SiMe_3), and the yield of what we presume to be [N_3N]Mo≡CPh (according to its C_3-symmetry and [N_3N]$^{3-}$ ligand chemical shifts in the proton NMR spectrum) is again low. After 5 days at 100 °C in toluene-d_8 a sample contained 13% [N_3N]Mo(CH_2Ph) and 40% [N_3N]Mo≡CPh (versus an internal standard); the fate of the remaining material could not be determined.

Heating [N_3N]MoMe to 120 °C for 24 h in toluene-d_8 did not yield any significant amount of [N_3N]Mo≡CH, a compound that can be prepared by another route (see later); [N_3N]MoMe simply slowly disappeared, and no decomposition products could be identified. This result should be compared with the decomposition of [N_3N]WMe to [N_3N]W≡CH at 120 °C, for which the calculated half-life is ∼10 s.[12] Therefore [N_3N]MoMe is approximately 4 orders of magnitude more stable than [N_3N]WMe at 120 °C with respect to decomposition to give a methylidyne complex. It is interesting to note that [N_3N]MoMe does not lose methane by C−H activation in the TMS group to give a complex that is stable under these conditions (see later).

Decomposition of [N_3N]Mo(CH_2R') to [N_3N]Mo≡CR′ is analogous to the faster and better documented decompositions of tungsten complexes of this type.[12] It is proposed that [N_3N]Mo(CH_2R') is converted into [N_3N]Mo(H)(CHR′) and that dihydrogen is lost from [N_3N]Mo(H)(CHR′) by a type of "α-hydrogen abstraction" reaction (eq 6).[23] We have shown that

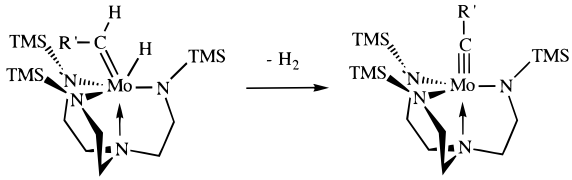

(6)

the rates of forming a cyclopentylidene hydride from [N_3N]Mo(cyclopentyl) and a cyclohexylidene hydride from [N_3N]Mo(cyclohexyl) can be relatively fast. Since the difference between the rates of α-elimination in [N_3N]Mo(cyclopentyl) and [N_3N]Mo(cyclohexyl) is already significant (∼10×), we suspect that the rates of forming [N_3N]Mo(H)(CHR′) complexes from various [N_3N]Mo(CH_2R') complexes also will differ dramatically. (See the Discussion.)

[N_3N]Mo($CH_2CH_2CH_2CH_3$) decomposes at 80 °C to give a mixture of paramagnetic [N_3N]MoH (see later) and [N_3N]Mo≡CPr (see later), while [N_3N]Mo(CH_2CH_3) decomposes to what we presume to be C_3-symmetric [N_3N]Mo≡CMe, in both cases as a consequence of competitive α,α-dehydrogenation (eq 6) and β hydride elimination followed by loss of olefin (eq 7).

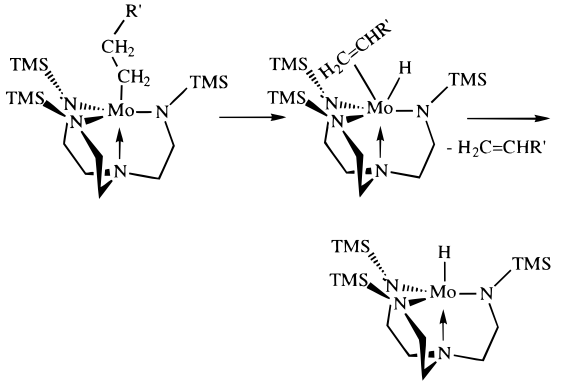

(7)

After heating a solution of [N_3N]MoBu for 2 days at 80 °C the ratio of [N_3N]MoBu to [N_3N]MoH to [N_3N]Mo≡CPr was 67:21:12; after 7 days it was 17:54:29. After heating a solution of [N_3N]Mo(CH_2CH_3) for 16 h at 80 °C the ratio of [N_3N]MoEt to [N_3N]MoH to [N_3N]Mo≡CMe was 60:28:12. [N_3N]Mo≡CPr can be made more practically from [N_3N]Mo(cyclobutyl) (see below) and [N_3N]MoH from [N_3N]Mo(cyclopentyl) (see below). Qualitatively the rate of formation of [N_3N]MoH from [N_3N]MoBu or [N_3N]MoEt is significantly less than from the analogous cyclopentyl or cyclohexyl complexes (see below), perhaps in part because a monosubstituted olefin is not lost as readily from the metal in a [N_3N]Mo(olefin)(H) intermediate as is a cyclic olefin. It is clear that for ethyl and butyl complexes the overall rate of forming [N_3N]MoH via the two-step process shown in eq 7 is approximately the same as the rate of forming an alkylidyne complex via the two-step process shown in eq 4.

[N_3N]Mo$^{13}CH_2CH_2CH_2CH_3$ was prepared and its decomposition monitored by ^{13}C NMR in a sealed NMR tube. A resonance was observed at 298.3 ppm, the same position as the α-carbon atom in [N_3N]Mo≡$CCH_2CH_2CH_3$ prepared by another method (see below), consistent with formation of virtually entirely [N_3N]Mo≡$^{13}CCH_2CH_2CH_3$. On the basis of relative intensities of resonances in the ^{13}C NMR spectrum, we estimate that <10% [N_3N]Mo≡$CCH_2CH_2{}^{13}CH_3$ ($\delta 13_C$ = 14.6 ppm) is

(24) Murdzek, J. S.; Schrock, R. R. *Carbyne Complexes*; VCH: New York, 1988.

present. Resonances for 1-butene also were consistent with formation of >90% $^{13}CH_2{=}CHCH_2CH_3$. This is the result to be expected if the metal cannot "walk" to the other end of the butyl chain (by forming [N_3N]Mo(*sec*-butyl) and [N_3N]Mo(2-butene)(H) intermediates) before 1-butene is lost. If an isomerization of this type *were* rapid relative to the rate of loss of 1-butene, then a 1:1 mixture of $^{13}CH_2{=}CHCH_2CH_3$ and $CH_2{=}CHCH_2{}^{13}CH_3$ would be obtained. Formation of only [N_3N]Mo$\equiv{}^{13}CCH_2CH_2CH_3$ is also consistent with no [N_3N]Mo($CH_2CH_2CH_2{}^{13}CH_3$) being formed before α,α-dehydrogenation.

When **2g** is heated it is converted into pale yellow [N_3N]-Mo≡CH (**3a**; eq 8), while **2h** is converted into [N_3N]Mo≡CCH_2-CH_2CH_3 (**3c**; eq 9). Both reactions are quantitative and can be followed conveniently by UV/vis spectroscopy at 540 and 558 nm, respectively, in toluene or THF. The reactions are first order through several half-lives and independent of concentration over a 40 °C temperature range. Rates in THF are within experimental error the same as those in toluene, as shown in Table 3 for **2g**. The rates of decomposition of **2g** and **2h** are comparable and more than 2 orders of magnitude faster than the rate of decomposition of [N_3N]Mo(neopentyl) to [N_3N]-Mo≡$CCMe_3$. (See calculated *k* values at 298 K in Table 3.) The reaction shown in eq 8 is the only practical way to prepare

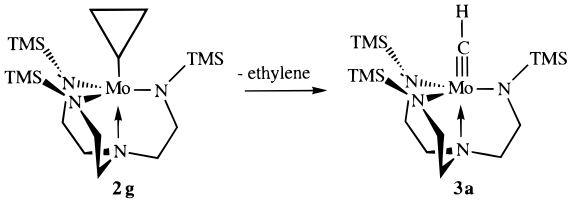

(8)

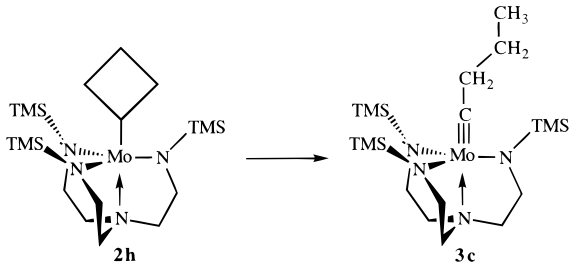

(9)

3a, since [N_3N]MoMe will not lose dihydrogen to give **3a**. The reaction shown in eq 9 is also the only practical way to prepare **3c**, since [N_3N]Mo(*n*-butyl) decomposes largely to [N_3N]MoH (see above). As mentioned earlier, rapid and reversible C−C bond cleavage in [N_3N]Mo(cyclopentyl) and [N_3N]Mo(cyclohexyl) is an alternative way to explain interconversion of exo and endo protons, but the relatively slow rate of C−C bond cleavage in **2g**,**h** would seem to preclude *rapid* C−C bond cleavage in less strained five- and six-membered rings in analogous compounds. Compound **3a**, like high oxidation state methylidyne complexes of the type W(CH)$(OR)_3$(donor),[24] is relatively stable toward bimolecular decomposition reactions, whereas W(CH)$(OR)_3$ complexes are not.[25]

Upon heating a solution of the cyclopentyl complex (**2i**), cyclopentene is lost and yellow, paramagnetic [N_3N]MoH (eq 10) is formed quantitatively, according to NMR spectra. It can be isolated in ~60% yield on a scale of ~1 mmol. When [N_3N]-MoD (see below) is dissolved in neat cyclopentene and the solution is heated to 50 °C for 18 h, no deuterium is incorporated into the cyclopentene, according to ^{2}H NMR acquired under

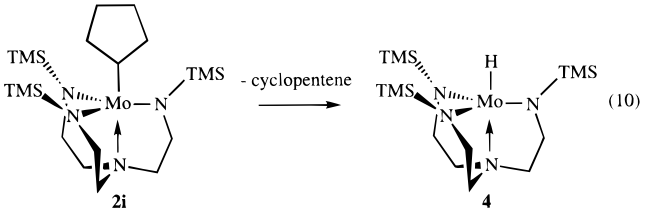

(10)

conditions where incorporation would be easily ascertained. Therefore the decomposition of **2i** is essentially irreversible. The $\Delta H^{\ddagger}$ and $\Delta S^{\ddagger}$ values for decomposition of **2i** are virtually the same as those for [N_3N]Mo(cyclopropyl) (Table 3). The hydride resonance could not be located in the NMR spectrum of [N_3N]MoH, but an M−H stretch could be found in the IR spectrum at 1681 cm^{-1}. [N_3N]MoH is best prepared by preparing **2i** in situ and heating the solution thereafter. [N_3N]-MoH shows the same type of temperature-dependent susceptibility as other compounds of this type, as shown in Figure 7 for [N_3N]MoD. A fit of these data to an equation[17,18] involving g (= 2), E (= 0.1 cm^{-1}), and D yielded a value of D = 22 cm^{-1} (R = 0.9993).

[N_3N]Mo(cyclohexyl) also decomposes cleanly to give [N_3N]-MoH, as determined by NMR and by following the reaction in toluene by UV/vis at 562 nm. The first-order conversion of [N_3N]Mo(cyclohexyl) into [N_3N]MoH was followed at five temperatures between 323 and 363 K, and the values of $\Delta H^{\ddagger}$ and $\Delta S^{\ddagger}$ from an Eyring plot are listed in Table 3. The decomposition of [N_3N]Mo(cyclohexyl) is ~10× slower than that of [N_3N]Mo(cyclopentyl). (At 298 K the rate constants are calculated to be 4.0×10^{-7} s^{-1} for [N_3N]Mo(cyclohexyl) and 5.3×10^{-6} s^{-1} for [N_3N]Mo(cyclopentyl).) At 343 K [N_3N]-Mo(C_6D_{11}) was found to decompose with $k = 3.0 \times 10^{-5}$ and 3.3×10^{-5} s^{-1}. Since the rate constant for decomposition of [N_3N]Mo(C_6H_{11}) at 343 K is calculated to be 10.7×10^{-5} s^{-1}, the isotope effect at that temperature is 3.4(2). A deuterium isotope effect of this magnitude is consistent with cleavage of a CH bond.

At 100 °C [N_3N]MoH begins to evolve dihydrogen to give the paramagnetic "[bitN_3N]Mo" complex shown in eq 11.

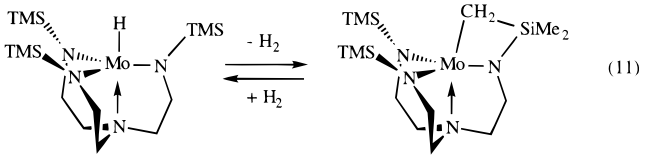

(11)

When [N_3N]MoH is heated to 105 °C in toluene-d_8 in an evacuated, sealed NMR tube, a 50/50 mixture of [N_3N]MoH and [bitN_3N] is observed after 22 h. Removal of the H_2 above this solution and further heating for another 22 h yields a 70/30 mixture of [bitN_3N] and [N_3N]MoH. Heating for another 24 h gave a 80/20 mixture. [bitN_3N]Mo reacts with D_2 slowly to give largely [N_3N]MoD in which a second deuterium is located in a TMS group, as shown by ^{2}H NMR spectra, thereby confirming that loss of hydrogen (eq 11) is reversible. However, both loss of hydrogen from [N_3N]MoH and reaction of [bitN_3N]-Mo with hydrogen are relatively slow. [bitN_3N]Mo has mirror symmetry, according to its ^{1}H NMR spectra. Its susceptibility versus temperature (Figure 7) is similar to other d^2 complexes discussed here, a fact that is consistent with magnetic behavior that does not depend on any significant structural change. A fit of these data to an equation[17,18] involving g (= 2), E (= 0.1 cm^{-1}), and D yielded a value of D = 31 cm^{-1} (R = 0.9993).

The most convenient laboratory synthesis of [bitN_3N]Mo is by reduction of [N_3N]MoCl with excess magnesium powder in

(25) Chisholm, M. H.; Folting, K.; Hoffman, D. M.; Huffman, J. C. *J. Am. Chem. Soc.* **1984**, *106*, 6794.

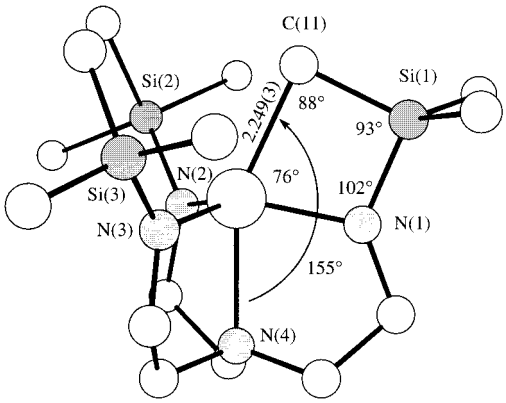

Figure 12. View of the structure of [bitN$_3$N]Mo.

THF in an evacuated vessel over a period of 7 days. The product is proposed to arise via loss of a hydrogen radical from **B** (eq 12), which is proposed to be in equilibrium with the

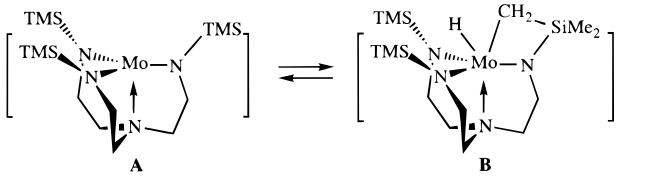

(12)

"monopyramidal" complex **A**, the product of reducing [N$_3$N]-MoCl by one electron followed by loss of chloride. One possible fate of the hydrogen radical is to combine with **A** to give [N$_3$N]MoH. In fact, [N$_3$N]MoH is a significant impurity in the reduction, but [bitN$_3$N]Mo can be separated from [N$_3$N]-MoH by crystallization. Another possible fate of the hydrogen radical is formation of dihydrogen, which we know reacts slowly with [bitN$_3$N]Mo to give [N$_3$N]MoH. Therefore the precise origin of [N$_3$N]MoH in the reduction reaction is not known.

An X-ray study showed [bitN$_3$N]Mo to have the structure shown in eq 11 (Figure 12, Table 1). The Mo−C(11) bond is somewhat longer than the Mo−L$_{ax}$ bonds in [N$_3$N]MoMe (**2a**) and [N$_3$N]Mo(cyclohexyl) (**2j**), but the M−N$_{eq}$ bond lengths and N$_{eq}$−Mo−N$_{eq}$ and Mo−N$_{eq}$−Si (except to Si(1)) bond angles are remarkably close to those found in **2a**,**j**. The Mo−N(4) bond length is significantly shorter than that in **2a**,**j**, but bond lengths and angles in general are consistent with a molecule whose coordination sphere is relatively uncrowded and undistorted. The absence of distortion in the MoN$_4$ core is somewhat surprising in view of the presence of the Mo−C−Si−N ring and relatively small N(4)−Mo−C(11) angle (155.16-(8)°). Although C−H activation in TMS amido complexes is relatively well-known,[26−28] X-ray structures of complexes that contain a MNSiC ring are rare. One such species is Zr[CH$_2$-SiMe$_2$N(SiMe$_3$)]$_2$(dmpe).[29] It contains two planar four-membered metallacyclic rings analogous to that found in [bitN$_3$N]Mo (C−Zr−N = 76°; Zr−N−Si − 97°; N−Si−C − 99°; Si−C−Zr = 87°).

[bitN$_3$N]Mo is not formed upon heating [N$_3$N]MoR complexes that are relatively stable toward decomposition by other pathways. For example, [N$_3$N]MoPh is quite stable thermally (decomposition is slow at 120 °C), and there is no evidence that [bitN$_3$N]Mo forms over a period of 24 h at 120 °C. Likewise, no [bitN$_3$N]Mo is formed when [N$_3$N]MoMe decomposes, as noted earlier.

Discussion

The phenomenon of β-hydride elimination to give an olefin hydride has dominated transition metal alkyl chemistry compared to α-elimination to give an alkylidene hydride.[30] Evidence for an equilibrium between an alkyl complex and alkylidene hydride has usually involved high oxidation state tungsten[31−33] or tantalum[34−38] alkyl complexes. In the Cp*$_2$Ta system observable Cp*$_2$Ta(CH$_2$)(H) was found to be in equilibrium with unobservable Cp*$_2$Ta(CH$_3$).[37] It was also shown that Cp*$_2$(H)Ta=C=CH$_2$ decomposed via intermediate Cp*(η^5-C$_5$-Me$_4$CH$_2$CH$_2$CH$_2$)Ta to the kinetic product, Cp*(η^5-C$_5$Me$_4$CH$_2$-CH$_2$CH)Ta(H), by α-elimination, and to the thermodynamic product, Cp*(η^5-C$_5$Me$_4$CH$_2$-η^2-CH=CH$_2$)Ta(H), by β-elimination.[38] It was noted that "the rate of α-H elimination is 10^8 times greater than the rate of β-H elimination" in this circumstance. However, it was also noted that "the generality of faster α-H elimination versus β-H elimination is questionable, since the transition state for β-H elimination in this system is highly strained, whereas that for α-H elimination is much less so." Finally, it was argued that "for a general alkyl ligand in the permethyltantalocene system, α-H elimination cannot be kinetically favored over β-H elimination by more than... a factor of ∼30 in rate at 25 °C." Similar statements could be made about many of the alkyl complexes reported here, although the validity and generality of such statements are limited by the experimental data available. It is generally assumed that an agostic interaction[20] between the metal and CH$_\beta$ or CH$_\alpha$ is on the pathway for β- or α-elimination, respectively, even though definitive evidence for α-agostic interactions in group VI d^0 complexes is still sparse.[21]

α-Abstraction in a dialkyl complex (to give alkane and an alkylidene complex)[23] is closely related to α-elimination, and an α-agostic activation of an α-proton in one of the alkyls is thought to precede α-abstraction. It has long been known that neopentyl complexes are most prone to α-abstraction, with (trimethylsilyl)methyl, benzyl, and especially methyl being progressively less so.[23] It was also noted in early studies that α-abstraction is faster in sterically crowded environments, e.g., when additional ligands coordinate to the metal.[23] Recently it has been shown that α-abstraction and β-abstraction can compete in [(Me$_3$SiNCH$_2$CH$_2$N)$_3$N]Ta(alkyl)$_2$ species,[39] that the rate of α abstraction can be enhanced by increasing the size of the alkyls in the apical "pocket",[40] and that α-abstraction to give an alkylidene can be forced to be virtually the only

(26) Simpson, S. J.; Andersen, R. A. *Inorg. Chem.* **1981**, *20*, 2991.
(27) Turner, H. W.; Simpson, S. J.; Andersen, R. A. *J. Am. Chem. Soc.* **1979**, *101*, 2782.
(28) Simpson, S. J.; Andersen, R. A. *Inorg. Chem.* **1981**, *20*, 3627.
(29) Planalp, R. P.; Andersen, R. A. *Organometallics* **1983**, *2*, 1675.
(30) Collman, J. P.; Hegedus, L. S.; Norton, J. R.; Finke, R. G. *Principles and Applications of Organotransition Metal Chemistry*; University Science Books: Mill Valley, CA, 1987.
(31) Cooper, N. J.; Green, M. L. H. *J. Chem. Soc., Chem. Commun.* **1974**, 209.
(32) Cooper, N. J.; Green, M. L. H. *J. Chem. Soc., Chem. Commun.* **1974**, 761.
(33) Cooper, N. J.; Green, M. L. H. *J. Chem. Soc., Dalton Trans.* **1979**, 1121.
(34) Turner, H. W.; Schrock, R. R. *J. Am. Chem. Soc.* **1982**, *104*, 2331.
(35) Turner, H. W.; Schrock, R. R.; Fellmann, J. D.; Holmes, S. J. *J. Am. Chem. Soc.* **1983**, *105*, 4942.
(36) Fellmann, J. D.; Schrock, R. R.; Traficante, D. D. *Organometallics* **1982**, *1*, 481.
(37) van Asselt, A.; Burger, B. J.; Gibson, V. C.; Bercaw, J. E. *J. Am. Chem. Soc.* **1986**, *108*, 5347.
(38) Parkin, G.; Bunel, E.; Burger, B. J.; Trimmer, M. S.; Asselt, A. v.; Bercaw, J. E. *J. Mol. Catal.* **1987**, *41*, 21.
(39) Freundlich, J. S.; Schrock, R. R.; Davis, W. M. *J. Am. Chem. Soc.* **1996**, *118*, 3643.
(40) Fruendlich, J. S.; Schrock, R. R.; Davis, W. M. *Organometallics* **1996**, *15*, 2777.

sterically tenable process by increasing the size of the silyl substituent in $[(R_3SiNCH_2CH_2N)_3N]Ta(alkyl)_2$ species from R = Me to R = Et. In a more crowded "pocket", the β-agostic interaction that precedes β-abstraction in the alkyl becomes sterically disfavored, while the α-agostic interaction that precedes α-abstraction at the same time is encouraged.

The preceding discussion would suggest that α-processes (abstraction or elimination) can be dramatically accelerated *at the expense of* β-processes (abstraction or elimination) and that steric (or "conformational") factors play a key role in determining the relative rates of α- versus β-processes in a given complex. Therefore, it is becoming increasingly clear that broad statements concerning the relative rates of α- versus β-processes simply cannot be justified, even for a given metal with the same ligand coordination sphere. Nevertheless, it seems relatively safe to say that competition between α- and β-processes will continue to be found among the earlier, heavier metals (Ta, Mo, W, Re) where multiple metal−carbon bonds (alkylidenes and alkylidynes) are relatively common.[23] Whether α-elimination is faster than β-elimination for later metals (e.g., iridium[41]) has yet to be investigated thoroughly.

We have observed that α-elimination is fast relative to β-elimination in two $[N_3N]$Mo(cycloalkyl) systems, even though no alkylidene hydride complex is observed in either case. To our knowledge any consequence of rapid and reversible α-elimination has never been observed *directly* before, perhaps largely because no net change in the alkyl itself occurs. Rapid α-elimination could be documented here in part because of the paramagnetic nature of the $[N_3N]$Mo(cycloalkyl) complexes and the resulting dispersion of all cycloalkyl resonances (including exo and endo resonances) in NMR spectra, a phenomenon that has proved useful in the coordination chemistry of paramagnetic coordination complexes for some time.[22] We suspect that α-elimination in some $[N_3N]$Mo(*n*-alkyl) complexes can also be "rapid" (e.g., 10^{-1} s^{-1} or greater), but perhaps only when the Mo−C_α-C_β angle is opened up as a consequence of steric interactions (e.g., in $[N_3N]$Mo(neopentyl)). Unfortunately, we have not been able to think of a way to measure the rate of conversion of, for example, $[N_3N]Mo(CH_2CMe_3)$ to $[N_3N]Mo(CHCMe_3)(H)$ to compare the rate of α-elimination with that found in $[N_3N]$Mo(cyclopentyl) and $[N_3N]$Mo(cyclohexyl). For alkyls in general the situation is complicated by competitive α-abstraction reaction (α,α-dehydrogenation) and β-hydride elimination processes. A plausible scenario is that the rate of α-elimination in $[N_3N]Mo(CH_2CMe_3)$ could be of the same order of magnitude as it is in $[N_3N]$Mo(cyclopentyl) or $[N_3N]$Mo(cyclohexyl) (i.e., 10 to 10^3 s^{-1} at 22 °C), but $[N_3N]Mo(CCMe_3)$ does not form readily because $[N_3N]Mo(CHCMe_3)(H)$ does not lose hydrogen rapidly enough to compete with the back reaction to reform $[N_3N]Mo(CH_2CMe_3)$. Therefore a plausible explanation as to why other $[N_3N]Mo(CH_2R)$ complexes decompose to $[N_3N]Mo{\equiv}CR$ complexes progressively less readily as the size of R decreases is that the equilibrium between $[N_3N]Mo(H)(CHR)$ and $[N_3N]Mo(CH_2R)$ complexes becomes prohibitively large, i.e., virtually no $[N_3N]Mo(H)(CHR)$ is present. The equilibrium between $[N_3N]Mo(H)(CHR)$ and $[N_3N]Mo(CH_2R)$ could become large either as a consequence of a precipitous drop in the rate of α-elimination or as a consequence of a dramatic increase of the rate of forming an alkyl complex from an alkylidene hydride complex. If it is the former, then α-elimination could even become rate limiting in the reaction in which an alkylidyne complex is formed from an alkyl complex, e.g., α,α-dehydrogenation in $[N_3N]$MoMe to form $[N_3N]Mo{\equiv}CH$. It is interesting to note that the overall relative ease of forming an alkylidyne complex via loss of H_2 from the alkyl (CH_2CMe_3 > CH_2SiMe_3 > CH_2Ph ≫ Me) is analogous to what has been observed qualitatively for α-hydrogen abstraction in tantalum dialkyl complexes to give alkylidene complexes.[23] Data for formation of alkylidyne complexes from alkylidene complexes[24] by α-hydrogen abstraction is more sketchy but in accord with a general trend toward more facile α-abstraction from bulkier alkylidenes.

The X-ray structures of the methyl and cyclohexyl $[N_3N]$MoR species illustrate semiquantitatively the differences in the degree of steric congestion within the trigonal pocket. These differences suggest that a greater rate of α-elimination *in part* could be traced to a relief of steric strain within the pocket. However, so many other factors must be taken into account that we can only in a very general sense feel secure in concluding that steric congestion increases the rate of α-elimination. In fact, the rate of α-elimination in the cyclohexyl complex is significantly *slower* than the rate of α-elimination in the cyclopentyl complex at 22 °C, even though one would expect steric congestion in the *ground* state of the cyclohexyl species to be *greater*. However, a greater degree of steric congestion in $[N_3N]$Mo(cyclohexylidene)(H) (versus $[N_3N]$Mo(cyclopentylidene)(H)) should oppose that trend and lead to a slower rate of α-elimination. Correlating the rates of β-elimination with steric congestion in either the ground state or in the olefin hydride intermediate species in these systems is also virtually impossible for similar reasons at this stage.

In contrast to the equilibria observed here, the equilibrium between $[N_3N]$W(cycloalkyl) and $[N_3N]$W(cycloalkylidene)(H) complexes has been observed to lie toward the latter for cyclopentyl[13] and cyclohexyl.[14] However, $[N_3N]$WMe is observable.[12] These results are consistent with a substantially slower rate of α-elimination in the methyl complex and/or a relatively small equilibrium constant for forming $[N_3N]W(CH_2)(H)$. The observation of tungsten(VI) alkylidene hydride complexes, but molybdenum(IV) alkyl complexes, could be explained using oxidation state and/or bond strength arguments. The fact that α,α-dehydrogenation reactions in $[N_3N]W(CH_2R)$ complexes are orders of magnitude faster than in the analogous $[N_3N]Mo(CH_2R)$ complexes also could be explained in terms of a higher concentration of alkylidene hydride in a W system versus an analogous Mo system. A more detailed discussion and relevant results may be found in a paper concerning $[N_3N]$W(alkyl) chemistry.[14]

It may be worth pointing out that we have assumed throughout this work that the $[N_3N]$ ligand is not directly involved in proton migration reactions, i.e., a proton does not migrate from carbon to nitrogen to produce a $[(Me_3SiNCH_2CH_2)_2N(CH_2CH_2NHSiMe_3)]^{2-}$ ligand. However, such a ligand has been observed in the analogous C_6F_5-substituted ligand system.[42] Therefore the possibility of forming an intermediate via proton migration to an amido nitrogen (e.g., eq 13) must be

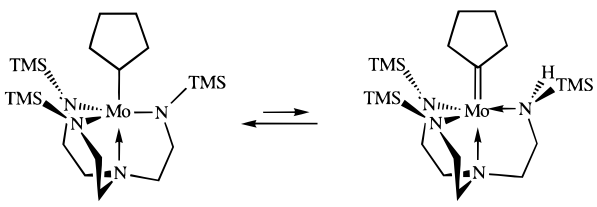

(13)

considered in a totally objective analysis. There is no change in oxidation state of the metal in such a reaction if we assume

(41) Burk, M. J.; McGrath, M. P.; Crabtree, R. H. *J. Am. Chem. Soc.* **1988**, *110*, 620.

(42) Rosenberger, C.; Schrock, R. R.; Davis, W. M. *Inorg. Chem.* **1997**, *36*, 123.

that the alkylidene is a dianion. A rapid process of this nature *could* explain interconversion of exo and endo protons in [N_3N]-Mo(cyclopentyl), *if* the alkylidene could rotate readily by 180° before the amido proton migrates back to the alkylidene carbon atom.

The carbon−carbon bond cleavage reactions that have been observed here for [N_3N]Mo(cyclopropyl) and [N_3N]Mo-(cyclobutyl) are surprisingly facile alternatives to CH bond cleavage reactions and, in fact, take place more readily than the overall rate of α,α-dehydrogenation in [N_3N]Mo(neopentyl). Carbon−carbon bond cleavage in cyclopropane rings that are external to the coordination sphere has much precedent in the literature,[30] and in some cases, C−C bond cleavage in a cyclopropyl ligand has been observed.[43] However, probably for thermodynamic reasons,[30] C−C bond cleavage in hydrocarbons or hydrocarbyl ligands with less π character in the C−C bond is rare.[44,45] We could find no example in the literature of C−C cleavage of a cyclobutyl ligand by a transition metal. Surprisingly, both the cyclopropyl and cyclobutyl systems manage to find a pathway to alkylidyne complexes. We speculate that a highly strained 1-metallacyclobutene complex (**A**) is the result of C−C cleavage in the cyclopropyl complex (eq 14). **A** also could be formed via reaction of the methylidyne

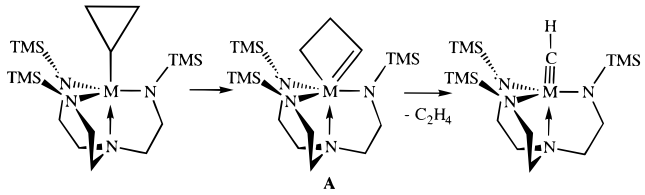

(14)

complex with ethylene, but that hypothetical reaction is still unknown for any high oxidation state alkylidyne complex.[24] Therefore it would not be surprising to find that **A** would eject ethylene to form the methylidyne complex. It is not known whether reversible C−H_β bond cleavage competes with C−C bond cleavage reactions in the cyclopropyl complex, as an appropriate $^{13}C_\alpha$ labeling experiment has not been carried out.

How a butylidyne complex forms from a cyclobutyl complex is more speculative. The reaction between [N_3N]WCl and cyclobutyllithium has been shown to yield the 1-tungstacyclopentene complex shown in eq 15,[14] and this species has been shown to rearrange cleanly to the butylidyne complex by what could be viewed as an α-hydrogen abstraction from an alkylidene ligand to give an alkylidyne ligand. Therefore we assume that rearrangement of the molybdenum cyclobutyl complex follows a similar pathway. However, there is no evidence that suggests that the [N_3N]Mo(cyclobutyl) complex interconverts rapidly and reversibly with the 1-molybdacyclopentene complex (eq 16), with the equilibrium lying well toward the cyclobutyl complex, and indeed, one would not expect C−C bonds to be cleaved and reformed nearly as readily as C−H bonds. The equilibrium shown in eq 16 could be observed in the NMR spectrum of [N_3N]Mo(cyclobutyl) if it were fast enough, as endo and exo protons would exchange in the process. Although we did not observe rapid exo/endo exchange of cyclobutyl protons in [N_3N]Mo(cyclobutyl), we cannot exclude the possibility, however unlikely it might be, that the equilibrium between [N_3N]M(cyclobutyl) and the 1-metallacyclopentene complex (eq 16) is fast on the chemical time scale, lies on the side of [N_3N]M(cyclobutyl) when M = Mo, and lies on the side of the 1-metallacyclopentene complex when M = W.

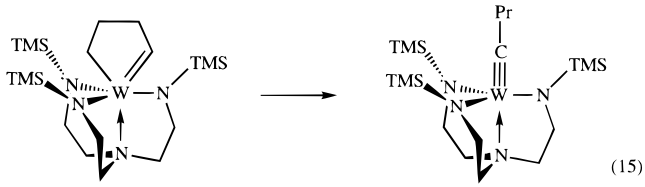

(15)

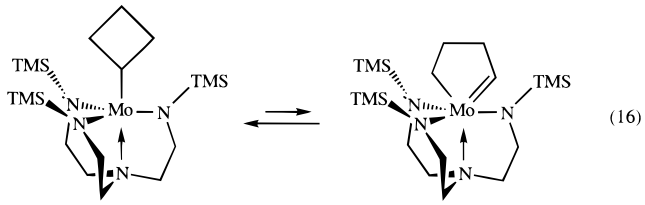

(16)

It is perhaps largely a consequence of the relative stability of the $[N_3N]^{3-}$ ligand system to various other decomposition reactions, especially *inter*molecular decomposition reactions and reactions involving ligand dissociation, that such a variety of intramolecular reactions can be observed. However, it is also somewhat surprising that the trimethylsilyl substituents do not undergo CH activation more readily than they do (e.g., to form [bitN_3N]Mo), as carbon−hydrogen bond activation in (usually hydride) complexes that contain one or more trimethylsilyl-substituted ligands has been observed in several systems, [26−28] including [N_3N]TiH.[3] Other possible decomposition reactions, e.g., loss of Me_3SiH[39] or degradation of the tren backbone by cleavage of an N_{ax}−C bond,[39,40] so far have not been identified in [N_3N]Mo alkyl complexes.

A potentially important feature of the alkyl systems studied here is the fact that they are all 16-electron, high-spin d^2 species. Many of the reactions discussed here, α−hydride elimination in particular, would seem to require an empty orbital in order to activate a C−H bond through an agostic interaction. However, so far there is no evidence that the rate of any of the reactions discussed here is limited as a consequence of the high spin ground-state alone, a possibility that was proposed in a preliminary communication.[13] Arguments concerning the degree to which spin state alone can alter the rate of an organometallic reaction have been in the literature for some time,[30,46−49] and the conclusion in every case so far has been that it cannot. However, since the vast majority of examples in the literature concern metals in lower oxidation states (usually carbonyl complexes), we will keep an open mind concerning the possibility that accessibility of some ^{1}A spin state (with an accompanying structural change) is an important feature of some of the chemistry of d^2 complexes of the type described here.

Experimental Section

General Details. All experiments were conducted under nitrogen in a Vacuum Atmospheres drybox, using standard Schlenk techniques, or on a high-vacuum line (<10^{-4} Torr). Pentane was washed with HNO_3/H_2SO_4 (5/95 v/v), sodium bicarbonate, and H_2O, stored over $CaCl_2$, and then distilled from sodium benzophenone under nitrogen. Regent grade ether, tetrahydrofuran, and benzene were distilled from sodium benzophenone under nitrogen. Toluene was distilled from molten sodium. Methylene chloride was distilled from CaH_2. All solvents were stored in the drybox over activated 4 Å molecular sieves.

(43) Periana, R. A.; Bergman, R. G. *J. Am. Chem. Soc.* **1984**, *106*, 7272.
(44) Halpern, J. *Acc. Chem. Res*, **1970**, *3*, 386.
(45) Bishop, K. C. *Chem. Rev.* **1976**, *76*, 461.
(46) Detrich, J. L.; Reinaud, O. M.; Rheingold, A. L.; Theopold, K. H. *J. Am. Chem. Soc.* **1995**, *117*, 11745.
(47) Gadd, G. E.; Upmacis, R. K.; Poliakoff, M.; Turner, J. J. *J. Am. Chem. Soc.* **1986**, *108*, 2547.
(48) Janowicz, A. H.; Bryndza, H. E.; Bergman, R. G. *J. Am. Chem. Soc.* **1981**, *103*, 1516.
(49) Parshall, G. W. *Catalysis. A Specialist Periodical Report*; The Chemical Society: London, 1977; Vol. 1, p 335.

Deuterated solvents were freeze−pump−thaw degassed and vacuum transferred from an appropriate drying agent, or sparged with argon and stored over sieves. NMR spectra are recorded in C_6D_6 unless noted otherwise. ^{1}H and ^{13}C data are listed in parts per million downfield from tetramethylsilane and were referenced using the residual protonated solvent peak. ^{19}F NMR are listed in parts per million downfield of $CFCl_3$ as an external standard. ^{2}H NMR spectra usually were obtained at 76.7 MHz and are referenced to external C_6D_6 (7.15 ppm). Coupling constants are given in hertz, and routine couplings are not listed. Elemental analyses (C, H, N) were performed on a Perkin-Elmer 2400 CHN analyzer in our own laboratory.

All organic compounds were received from commercial suppliers and were used as received. $MoCl_4(THF)_2$,[50] $MoCl_3(THF)_3$,[50] cyclohexyllithium,[51] and ethyllithium[52] were prepared according to published procedures. Benzyllithium was prepared from tribenzyltin chloride and methyllithium by the literature procedure.[53] Cyclopentyllithium and cyclobutyllithium were prepared from the chloride or bromide and lithium powder in pentane. Cyclopropyllithium was prepared from the bromide and lithium powder in diethyl ether. Perdeuteriocyclohexyl chloride was prepared from commercially available $C_6D_{11}OH$ and DCl as described in the literature.[54] 1-Deuteriocyclopentyllithium was prepared by reduction of cyclopentanone with lithium aluminum deuteride followed by treatment with Ph_3PBr_2 in DMF.[55] The bromide was converted to the lithium reagent by reaction with lithium powder in refluxing hexane. The lithium reagent was recrystallized from pentane before use. $Li^{13}CH_2CH_2CH_2CH_3$ was prepared by treating $^{13}CO_2$ with *n*-PrMgCl, reducing the acid with $LiAlH_4$ to the alcohol, chlorinating the alcohol with $SOCl_2$ in hexane, and finally treating the chloride with lithium wire in the usual manner; overall yield ∼20%.

In UV/vis studies the following equation was employed to follow the disappearance of an alkyl species: $\ln[(\lambda_o - \lambda_\infty)/(\lambda - \lambda_\infty)] = kt$, where λ_o = absorbance at wavelength λ at time 0, λ_∞ = absorbance at wavelength λ at infinite time, and λ = absorbance at wavelength λ at time *t*.

[N_3N]MoCl (1a). Method (a). $MoCl_4(THF)_2$ (2.53 g, 6.63 mmol) was added to a THF (∼150 mL) solution of $Li_3[N_3N]$ (3.50 g, 9.13 mmol), and the reaction mixture was stirred for 6 h. The resulting dark-brown solution was evaporated to dryness, and the residue was repeatedly extracted with pentane (500 mL). The pentane extract was filtered through Celite, and the volume was reduced in vacuo until orange crystals formed. The mixture was then chilled at −40 °C for 1 h, and the orange crystals were collected by filtration and washed quickly with cold pentane (2 × 10 mL). The crude product was recrystallized from diethyl ether to give bright orange crystals: yield 1.34 g (41%); ^{1}H NMR δ 5.73 (br s), −23.6 (br s), −99.2 (br s). Anal. Calcd for $C_{15}H_{39}N_4ClMoSi_3$: C, 36.68; H, 8.00; N, 11.41. Found: C, 36.63; H, 7.97; N, 10.90.

Method (b). A mixture of $MoCl_3(THF)_3$ (1.10 g, 2.63 mmol) and $Li_3[N_3N]$ (1.10 g, 2.63 mmol) in 80 mL of diethyl ether was stirred at room temperature for 4 h. The reaction mixture was filtered and the solid washed with 10 mL of diethyl ether. The volume of the filtrate was reduced to ∼5 mL in vacuo, and 10 mL of pentane was added. The solution was chilled to −40 °C overnight, and the orange-brown solid was filtered off and recrystallized twice from a mixture of diethyl ether and pentane: yield 0.31 g (24%).

[N_3N]Mo(OTf) (1b). [N_3N]MoCl (0.50 g, 1.02 mmol) and Cp_2FeOTf (0.375 g, 1.12 mmol) were added to 25 mL of dichloromethane, and the resulting solution was stirred for 6 h at 22 °C. The volume was reduced by one-third in vacuo, and 40 mL of diethyl ether was added. The mixture was chilled to −40 °C for several hours, and pink crystals were filtered off and dried in vacuo: yield 0.38 g (62%); ^{1}H NMR δ 11.0 (s, TMS), −42 (br s), −60 (br s). Anal. Calcd for $C_{16}H_{39}N_4F_3MoO_3SSi_3$: C, 31.78; H, 6.50, N, 9.26. Found: C, 31.78; H, 6.28; N, 9.78.

[N_3N]Mo(CH_3) (2a). A solution of **1a** (0.20 g, 0.41 mmol) in ∼25 mL of THF was treated with LiMe (291 μL, 0.41 mmol, 1.4 M in ether) at 25 °C. The reaction mixture was stirred for 3 h, and the solvent was removed in vacuo. Pentane (∼30 mL) was added to the reaction residue, and the extract was filtered through Celite to remove LiCl. The volume of the filtrate was then reduced to ∼3 mL in vacuo, and the concentrated solution was chilled to −40° to yield red crystals of the product. The product was collected by decantation of the mother liquor and dried in vacuo: yield 0.17 g in two crops (91%); ^{1}H NMR δ +7.77 ($SiMe_3$), −25.00 (NCH_2), −83.24 (NCH_2); λ_{max} = 486 nm in toluene, ϵ = 680 M^{-1} cm^{-1}; μ = 2.9 μ_B at 25 °C (Evan's method). Anal. Calcd for $C_{16}H_{42}N_4MoSi_3$: C, 40.82; H, 8.99, N, 11.90. Found: C, 40.87; H, 9.17; N, 12.11.

The chemical shifts for the methylene groups in [N_3N]MoMe (in toluene-d_8) are as follows (*T* (K), shift 1, shift 2): 363.16, −19.76, −62.29; 353.16, −20.57, −64.82; 343.16, −21.40, −67.52; 333.16, −22.23, −70.40; 323.16, −23.12, −73.58; 313.16, −24.06, −76.93; 303.16, −24.97, −80.34; 293.16, −26.11, −84.79; 283.16, −27.16, −89.27; 273.16, −28.18, −94.25; 263.16, −29.45, −99.52; 253.16, −30.67, −105.54; 243.16, −32.15, −112.24. These data were used to generate the plots shown in Figure 8b.

[N_3N]Mo(CH_2CH_3) (2b). Ethyllithium (21 mg) was added to a solution of [N_3N]MoCl (134 mg, 0.27 mmol) in 10 mL of ether. The color changed immediately to deep purple. The reaction mixture was stirred for 2 h, after which the solvents were removed in vacuo and the resulting solid was extracted with a minimum amount of pentane. The solution was cooled to − 40 °C to yield purple crystals: yield 100 mg (76%); ^{1}H NMR (toluene-d_8) 9.3 ($SiMe_3$), −25.05 (NCH_2), −51.5 (ethyl CH_3), −60.0 (NCH_2).

[N_3N]Mo($CH_2CH_2CH_2CH_3$) (2c). Compound **2c** was synthesized as described for **2b** from *n*-butyllithium in hexane (1.1 equiv) and [N_3N]-MoCl (120 mg, 0.24 mmol) in 5 mL of ether; yield 88 mg (70%): ^{1}H NMR (toluene-d_8) 9.3 ($SiMe_3$), −26 (NCH_2), − 47 (butyl CH_2), −59 (NCH_2).

[N_3N]Mo(CH_2Ph) (2d). Compound **2d** was synthesized as described for **2b** from 80 mg (0.16 mmol) of [N_3N]MoCl and 38 mg of $LiCH_2Ph(ether)_{1.25}$: yield 84 mg (94%); ^{1}H NMR (toluene-d_8) 10.92 (s, 1, H_p), 10.53 (s, 2, H_m), 9.18 ($SiMe_3$), −24.8 (NCH_2), − 63 (NCH_2); λ_{max} = 504 nm in toluene.

[N_3N]Mo(CH_2SiMe_3) (2e). Compound **2e** was prepared as described for **2a** from 108 mg (0.21 mmol) of [N_3N]MoCl and 34 mg (0.36 mmol) of $LiCH_2TMS$: yield 91 mg (76%); ^{1}H NMR (toluene-d_8) 8.5 (TMS), 1.28 (TMS), − 20.1 (NCH_2), −34.7 (NCH_2); $\lambda_{max(1)}$ = 496 nm, $\lambda_{max(2)}$ = 640 nm in toluene or THF. Anal. Calcd for $C_{19}H_{50}N_4Si_4Mo$: C, 42.03; H, 9.28, N, 10.32. Found: C, 42.05; H, 9.56; N, 10.20.

[N_3N]Mo(CH_2CMe_3) (2f). This complex was prepared from **1a** (0.50 g, 1.02 mmol) in THF (∼50 mL) and $LiCH_2CMe_3$ (0.12 g; 1.52 mmol) at 25 °C and was isolated as described for **2a**: yield 0.35 g (65%); ^{1}H NMR 8.8 ($SiMe_3$), −0.5 (s, *t*-Bu), −15.3 (NCH_2), −20.6 (NCH_2); $\lambda_{max(1)}$ = 480 nm, $\lambda_{max(2)}$ = 688 nm in toluene. Anal. Calcd for $C_{20}H_{50}N_4MoSi_3$: C, 45.60; H, 9.57, N, 10.63. Found: C, 45.51; H, 9.68; N, 10.69.

The conversion of [N_3N]Mo(CH_2CMe_3) into [N_3N]Mo≡$CCMe_3$ was followed by visible spectroscopy in toluene at 480 and 688 nm through at least three half-lives. (Identical results were obtained at each wavelength.) The rate constants (in units of 10^{-4} s^{-1}) obtained at temperature *T* (in K) were 0.50 (363), 1.70 (374), 4.38 (385), and 9.41 (394). A plot of $\ln(k/T)$ versus $1/T$ gave $\Delta H^\ddagger$ = 25 973 cal mol^{-1} and $\Delta S^\ddagger$ = −6.94 eu with an *R* value of 0.9988. The exact values were used to calculate *k* at temperature *T*.

[N_3N]Mo(cyclopropyl) (2 g). This compound was prepared from 126 mg (0.26 mmol) of [N_3N]MoCl in 10 mL of diethyl ether and a −10 °C solution of 64 mg (0.38 mmol) of cyclopropyllithium in 5 mL of diethyl ether. The reaction mixture was stirred at −10 °C overnight, during which the color changed from orange to deep purple. The solvent was evaporated, and the residue was extracted with cold (−40 °C) pentane. The volume of the filtrate was reduced to ∼1 mL in vacuo, and the solution was stored at −40 °C. After 2 days purple crystals were collected: yield 70 mg (55%); ^{1}H NMR δ 21 (cyclopropyl CH_2), 10.9 ($SiMe_3$), −27.9 (NCH_2), −47.6 (NCH_2), −93.8 (cyclopropyl CH); λ_{max} = 540 nm in toluene. Anal. Calcd for $C_{18}H_{44}N_4MoSi_3$: C, 43.52; H, 8.93; N, 11.28. Found: C, 43.58; H, 9.11; N, 11.15.

(50) Dilworth, J. R.; Richards, R. L. *Inorg. Synth.* **1990**, *28*, 33.
(51) Zerger, R.; Rhine, W.; Stucky, G. *J. Am. Chem. Soc.* **1974**, *96*, 6048.
(52) Bryce-Smith, D.; Turner, E. E. *J. Chem. Soc.* **1953**, 861.
(53) Seyferth, D.; Suzuki, R.; Murphy, C. J.; Sabet, C. R. *J. Organomet. Chem.* **1964**, *2*, 431.
(54) Perlman, D.; Davidson, D.; Bogert, M. T. *J. Org. Chem.* **1936**, *1*, 288.
(55) Wiley: G. A.; Hershkowitz, R. L.; Rein, B. M.; Chung, B. C. *J. Am. Chem. Soc.* **1964**, *86*, 964.

Decomposition of [N_3N]Mo(cyclopropyl) was followed in toluene by UV/vis spectroscopy at 540 nm; the values for k ($\times 10^{-4}$ s^{-1}) at temperature T (K) were 0.608 (313), 1.88 (323), 4.99 (333), 14.0 (343). A plot of ln(k/T) versus 1/T gave $\Delta H^{\ddagger} = 21\,506$ cal/mol and $\Delta S^{\ddagger} = -9.20$ eu with an R value of 0.9998. In THF the values for k ($\times 10^{-4}$ s^{-1}) at temperature T (K) were 0.147 (303), 0.490 (313), 0.838 (318), 2.44 (328), 3.98 (333). A plot of ln(k/T) versus 1/T gave $\Delta H^{\ddagger} = 21\,400$ cal mol^{-1} and $\Delta S^{\ddagger} = -10.02$ eu with an R value of 0.9999.

[N_3N]Mo(cyclobutyl) (2b). Cyclobutyllithium (14 mg, 0.23 mmol) was added to a solution of 93 mg (0.19 mmol) of N_3NMoCl in 10 mL of diethyl ether at −40 °C. The solution turned purple immediately. The solution was warmed to room temperature and was stirred for 1 h. The solvent was evaporated, and the residue was extracted with pentane and the extract was filtered. The volume of the extract was reduced to ∼1 mL in vacuo. Purple crystals were obtained after standing the solution overnight at − 40 °C: yield 30 mg (31%); ^{1}H NMR at −10 °C δ 33.9 (cyclobutyl), 13.1 ($SiMe_3$), −29.3 (NCH_2), −39.6 (br s, cyclobutyl CH_2), −40.4 (cyclobutyl), −107.8 (cyclobutyl); $\lambda_{max} = 558$ nm in toluene. Anal. Calcd for $C_{19}H_{46}N_4MoSi_3$: C, 44.68; H, 9.08; N, 10.97. Found: C, 44.40; H, 8.68; N, 10.79.

Conversion of [N_3N]Mo(cyclobutyl) into [N_3N]Mo≡$CCH_2CH_2CH_3$ was followed in toluene by UV/vis spectroscopy at 558 nm; the values for k ($\times 10^{-4}$ s^{-1}) at temperature T (K) were 0.110 (303), 0.443 (313), 1.54 (323), 5.03 (333), 13.8 (343). A plot of ln(k/T) versus 1/T gave $\Delta H^{\ddagger} = 24\,368$ cal/mol and $\Delta S^{\ddagger} = -0.07$ eu with $R = 0.9998$. In THF the values for k ($\times 10^{-4}$ s^{-1}) at temperature T (K) were 0.349 (313) and 3.98 (333).

[N_3N]Mo(cyclopentyl) (2i). A solution of cyclopentyllithium (155 mg, 2.02 mmol) dissolved in 10 mL of pentane was added to a solution of **1a** (498 mg, 1.01 mmol) in 25 mL of ether in a 100 mL flask. The solution changed color immediately to purple. After 1 h at room temperature, the volatile materials were removed in vacuo and the residue was extracted with minimum (∼5 mL) pentane. This extract was concentrated to ∼2 mL and cooled to −40 °C to give purple crystals (250 mg, 47%): ^{1}H NMR δ 21.2 (cyclopentyl), 15.3 (cyclopentyl), 10.2 ($SiMe_3$), −24.0 (NCH_2), −35.6 (NCH_2), −48.8 (cyclopentyl), −58.8 (cyclopentyl); $\lambda_{max} = 562$ nm in toluene. Adequate analytical data could not be obtained, we believe as a consequence to the facile decomposition of this compound to [N_3N]MoH.

The conversion was followed in toluene by UV/vis at 562 nm. The values for k ($\times 10^{-4}$ s^{-1}) at temperature T (K) are 0.363 (313), 1.188 (323), 3.197 (333), and 8.465 (343). A plot of ln(k/T) versus 1/T gave $\Delta H^{\ddagger} = 21\,631$ cal/mol and $\Delta S^{\ddagger} = -9.78$ eu with $R = 0.9997$.

[N_3N]Mo(1-cyclopentenyl) (2j). Cyclopentenyllithium (446 μL of a 1.7 M solution, 0.759 mmol) was added to a solution of 250 mg (0.506 mmol) of [N_3N]MoCl in 40 mL of ether. After 1 h, the volatile components were removed in vacuo and the yellow solid was extracted with 10 mL of pentane. The extract was filtered through Celite and cooled to −40 °C to yield 175 mg (0.334 mmol, 66%) of deep red crystals: ^{1}H NMR δ 18.5 (s, 2, cyclopentenyl CH_2), 11.1 (s, 27, TMS), −24.8 (s, 6, NCH_2), −60.5 (s, 6, NCH_2). Anal. Calcd for $C_{20}H_{46}N_4Si_3Mo$: C, 45.95; H, 8.84; N, 10.72; Found: C, 45.90; H, 8.78; N, 10.75.

[N_3N]Mo(cyclohexyl). Cyclohexyllithium (19 mg (0.21 mmol) was added to a solution of 92 mg (0.19 mmol) of **1a** in 10 mL of ether. The solution turned deep purple immediately. After 1 h, the solvent was removed in vacuo and the residue was extracted with pentane. Cooling the extract to −40 °C afforded 81 mg (80%) of purple crystals: ^{1}H NMR δ 15.58 (cyclohexyl CH_2), 10.04 ($SiMe_3$), 6.14 (cyclohexyl CH_2), 1.70 (cyclohexyl CH_2), −1.73 (cyclohexyl CH_2), −21.70 (NCH_2), −34.97 (NCH_2), −39.81 (cyclohexyl CH_2), −48.51 (cyclohexyl CH_2).

The conversion of [N_3N]Mo(C_6H_{11}) into [N_3N]MoH was followed in toluene by UV/vis at 562 nm. The first-order rate constants (in units of 10^{-4} s^{-1}) at temperature (T, K) at 323 K and k were found to be 0.127 (323), 0.428 (333), 1.07 (343), 3.68 (353), and 9.64 (363). A plot of ln(k/T) versus 1/T gave $\Delta H^{\ddagger} = 24\,501$ cal/mol and $\Delta S^{\ddagger} = -5.27$ eu with $R = 0.9989$. At 343 K the rate constant for decomposition of [N_3N]Mo(C_6H_{11}) was calculated to be 1.07×10^{-4} s^{-1}, while [N_3N]-Mo(C_6D_{11}) was found in two experiments to be 3.0×10^{-5} and 3.3×10^{-5} s^{-1} for a $k_H/k_D = 3.4(2)$.

The rate of α-elimination in [N_3N]Mo(C_6D_{11}) was determined by variable-T NMR as shown in Figure 11b and described in the text. Values for k are 606 s^{-1} at 331 K, 1273 s^{-1} at 346 K, and 1555 s^{-1} at 352 K. Virtually identical values were obtained for a sample that was one-half the concentration (0.05 M). By performing a similar experiment at 46.02 MHz three different points were obtained: 378 s^{-1} at 324, 755 s^{-1} at 339 K, and 955 s^{-1} at 343 K. A plot ln(k/T) versus 1/T for these six points gave $\Delta H^{\ddagger} = 10\,588$ cal mol^{-1} and $\Delta S^{\ddagger} = -14.19$ eu with $R = 0.9880$. Using these values, k at 337 K was calculated to be 696 s^{-1}. From the data shown in Figure 11a the rate constant for α-elimination in [N_3N]Mo(C_6H_{11}) was found to be 2155 s^{-1} at 337 K. The isotope effect at 337 K is therefore $k_H/k_D = 3.1(2)$.

[N_3N]Mo(phenyl) (2k). Phenyllithium (10 mg, 0.1 mmol) was added to a cold solution of 40 mg (0.08 mmol) of [N_3N]MoCl in 5 mL of diethyl ether. The solution was stirred overnight. The solvents were removed from the reaction mixture in vacuo, and the residue was extracted with pentane. The volume of the pentane extract was reduced in vacuo to 2 mL, and after 2 h at −30 °C, 30 mg (70%) of orange crystals was collected: ^{1}H NMR δ 64.2 (br s, Ph), 10.8 ($SiMe_3$), −23.9 (NCH_2), −67.0 (NCH_2). Anal. Calcd for $C_{21}H_{44}N_4MoSi_3$: C, 47.34; H, 8.32; N, 10.52. Found: C, 47.55; H, 8.18; N, 10.58.

[N_3N]Mo≡CH (3a). A solution of [N_3N]Mo(cyclopropyl) in ether was stirred at room temperature for 16 h. The color changed from deep purple to light brown. The solvent was evaporated, and the resulting powder was dissolved in a minimum amount of pentane. Crystallization at −30 °C gave pale yellow crystals: yield 75%; ^{1}H NMR 5.54 (CH), 3.37 (NCH_2), 2.15 (NCH_2), 0.48 ($SiMe_3$); ^{13}C NMR (toluene-d_8) δ 284.3 (CH), 53.2 (CH_2), 52.4 (CH_2), 4.5 (TMS). Anal. Calcd for $C_{16}H_{40}N_4MoSi_3$: C, 41.00; H, 8.60; N, 11.95. Found: C, 41.26; H, 8.65; N, 12.16.

[N_3N]Mo≡CPr (3c). [N_3N]Mo(cyclobutyl) (124 mg, 0.243 mmol) was dissolved in 5 mL of toluene, and the solution was heated in a sealed tube to 60 °C for 2 h. The toluene was removed in vacuo, and the residue was dissolved in a minimum amount of pentane. The pentane solution was cooled to −40° to give brown crystals of the product after 24 h: yield 107 mg in two crops (86%); ^{1}H NMR δ 3.50 (m, 2, CH_2), 3.41 (t, 6, NCH_2N), 2.13 (t, 6, NCH_2N), 2.05 (m, 2, CH_2), 0.86 (t, 3, CH_3), 0.50 (s, 27, TMS); ^{13}C{^{1}H} NMR δ 4.6 (TMS), 14.6 (CH_3), 23.4 (CH_2), 52.5 (NCH_2N), 53.8 (CH_2), 298.3 (Mo≡C). Anal. Calcd for $C_{19}H_{46}N_4Si_3Mo$: C, 44.68; H, 9.08; N, 10.97. Found: C, 44.39; H, 9.16; N, 11.06.

[N_3N]Mo≡$CCMe_3$ (3f). Compound **3f** was identified in solution as the sole product of decomposition of [N_3N]Mo(CH_2CMe_3) (vide supra): ^{1}H NMR (toluene-d_8) 3.2 (NCH_2), 2.18 (NCH_2), 1.57 (*t*-Bu), 0.37 (TMS); ^{13}C NMR (toluene-d_8) 316.08 (*C*-*t*-Bu), 56.88 (NCH_2), 54.16 (*C*CMe_3), 51.56 (NCH_2), 32.74 (*t*-Bu), 3.84 (TMS).

[N_3N]Mo≡CMe (3b), [N_3N]Mo≡CPh (3d), and [N_3N]Mo≡$CSiMe_3$ (3e) were observed only in solution by proton NMR. Although their identity does not seem to be in doubt, proof in the form of a ^{13}C NMR spectrum was not practical for experimental reasons, primarily the low percentage of alkylidyne complex in the product mixture.

[N_3N]MoH. A solution of [N_3N]Mo(C_5H_9) (150 mg, 0.286 mmol) in 10 mL of benzene was placed in a 100 mL Pyrex vessel which was sealed and heated at 45 °C for 24 h. The volatile materials were removed in vacuo, and the resulting yellow crystalline material was extracted with minimum pentane (∼5 mL). The extract was filtered through a 1 cm plug of Celite, and the volume of the solution was reduced by one-half in vacuo. The solution was stored at −35 °C for 1 day to produce yellow-orange needles: yield 75 mg (0.164 mmol, 58%); ^{1}H NMR δ 15.3 ($SiMe_3$, $w_{1/2} = 67$), −16.9 (NCH_2, $w_{1/2} = 306$), −117.6 (NCH_2, $w_{1/2} = 462$); IR (Nujol) cm^{-1} 1681 (m, ν_{MoH}). Anal. Calcd for $C_{15}H_{40}N_4Si_3Mo$: C, 39.45; H, 8.83 N; 12.27. Found: C, 39.95; H, 8.46; N, 12.06.

[bitN_3N]Mo. ($Me_3SiNCH_2CH_2)_3$N]MoCl (500 mg, 1.02 mmol) was dissolved in 13 mL THF and placed in a bomb. Magnesium powder (30 mg, 1.23 mmol) was added, and the bomb was sealed. The vessel was subjected to three freeze−pump−thaw cycles to remove any dinitrogen present, and the solution was stirred under vacuum. After 7 days, the solvent was removed and the residue extracted with 15 mL of pentane and filtered to give a blood-red solution. The pentane was removed to give the crude product as a red solid (420 mg) that was (according to its NMR spectrum) a 1:4 mixture of [N_3N]MoH and [bitN_3N]Mo. The crude yield of [bitN_3N] (in the mixture) therefore is

72%. Pure [bitN_3N]Mo was obtained by recrystallization of the crude product from hexamethyldisiloxane**:** ^{1}H NMR δ 18.58 (CH_2), 14.81 ($SiMe_3$), 1.10 ($SiMe_2$), −18.95 (CH_2), −20.26 (CH_2), −98.65 (CH_2), −103.55 (CH_2), −125.06 (CH_2). Anal. Calcd for $C_{15}H_{38}N_4Si_3Mo$: C, 39.62; H, 8.42; N, 12.32. Found: C, 39.74; H, 8.73; N, 12.39.

[N_3N]MoD. [bitN_3N]Mo (95 mg, 0.21 mmol) were dissolved in 5 mL of THF and placed in a glass bomb with a stirring bar. The vessel was sealed and subjected to two freeze−pump−thaw cycles. D_2 (1 atm) was introduced and the solution stirred for 2 days, during which time the color of the solution changed from blood-red to yellow. The solvent was removed and the solid recrystallized from pentane as yellow needles; the yield was quantitative: ^{2}D NMR (C_6H_6) δ 16.48 ($Si(CH_3)_2$-CH_2D, line width = 6 Hz).

X-ray Structure of [N_3N]Mo(triflate). The structure was solved at 188 K using a Siemens SMART/CCD diffractometer (see the Supporting Information): empirical formula $C_{16}H_{39}F_3N_4O_3SSi_3Mo$, FW = 604.78, space group $Pna2_1$, a = 20.951(4) Å, b = 10.999(2) Å, c = 12.050(2) Å, V = 2776.7(10) Å,^{3} Z = 4, D_{calc} = 1.447 mg/m^3.

X-ray Structure of [N_3N]Mo(CD_3). The structure was solved at 188 K using a Siemens SMART/CCD diffractometer (see the Supporting Information): empirical formula $C_{16}H_{39}D_3N_4Si_3Mo$, FW = 473.77, space group Cc, a = 17.352(10) Å, b = 9.6851(2) Å, c = 9.445(3) Å, β = 110.6210(10)°, V = 2508.00(7) Å,^{3} Z = 4, D_{calc} = 1.255 mg/m^3.

X-ray Structure of [N_3N]Mo(cyclohexyl). The structure was solved at 188 K using a Siemens SMART/CCD diffractometer (see the Supporting Information): empirical formula $C_{21}H_{50}N_4Si_3Mo$, FW = 538.86, space group $P\bar{6}$, a = 20.820(6) Å, b = 20.820(6) Å, c = 11.680(5) Å, V = 4385(3) Å,^{3} Z = 6, D_{calc} = 1.224 mg/m^3.

X-ray Structure of [bitN_3N]Mo. The structure was solved at 188 K using a Siemens SMART/CCD diffractometer (see the Supporting Information): empirical formula $C_{15}H_{38}N_4Si_3Mo$, FW = 454.70, space group $P2_1/n$, a = 8.972(3) Å, b = 17.308(4) Å, c = 15.398(3) Å, β = 100.61(3)°, V = 2350.2(11) Å,^{3} Z = 4, D_{calc} = 1.285 mg/m^3.

Solid-State Magnetic Susceptibility Measurements. SQUID experiments were performed at 5 kG on a Quantum Design 5.5 T instrument running MSRP2 software. Samples were prepared in an N_2-filled drybox. A gelatin capsule and 2.2 × 1.9 cm piece of parafilm were weighed. The capsule was then loaded with the sample, and the parafilm was folded and packed on top using plastic tongs. The capsule was closed and weighed again to determine the sample mass. It was then suspended in a straw. The straw was placed in a plastic bottle with a screw cap and the bottle was tightly sealed. At the instrument the straw was quickly attached to the sample rod and transferred to the helium atmosphere. Measurements were taken in 1° intervals from 5 to 10 K, 2° intervals from 12 to 20 K, 3° intervals from 23 to 50 K, 5° intervals from 55 to 100 K, 10° intervals from 110 to 200 K, and 20° intervals from 220 to 300 K. A background measurement of an empty gel capsule, parafilm square, and straw was taken over the entire temperature range and subtracted from the experimental values at each temperature. The susceptibility at each temperature also was corrected for the diamagnetic contribution by the ligands using Pascal's constants.

Acknowledgment. We thank the National Science Foundation for research support (CHE 91 22827) and for funds to help purchase a departmental Siemens SMART/CCD diffractometer. N.C.M-Z. thanks Ciba-Geigy for a Ciba-Geigy Jubiläums Stiftung and Jake Parrott (RSI program) for assistance in UV/vis measurements. S.W.S. thanks M. G. Fickes and R.R.S. thanks D. Nocera for helpful discussions.

Supporting Information Available: Labeled ORTEP drawing, crystal data and structure refinement, atomic coordinates, bond lengths and angles, and anisotropic displacement parameters, for [N_3N]Mo(triflate) (**1b**), [N_3N]Mo(CD_3) (**2a**-d_3), [N_3N]-Mo(cyclohexyl) (**2j**), and [bitN_3N]Mo, and solid-state susceptibility data for selected compounds (27 pages). An X-ray crystallographic file, in CIF format, is available through the Internet only. See any current masthead page for ordering and Internet access instructions.

JA970697X